Variable Star Section of Czech Astronomical Society and Valašské Meziříčí Observatory

Proceedings of the 40th Conference on Variable Stars Research

Valašské Meziříčí Observatory, Czech Republic, EU

14th – 17th November 2008,

Chief editor **Radek Kocián**

Participants of the conference in front of the observatory

TABLE OF CONTENT

A note:

The scientific content of the proceeding contributions has been refereed by the conference proceedings editors, not by the OEJV editorial board.

INTRODUCTION

Each year in November, when the full moon makes variable star observing difficult, the Variable Star and Exoplanet Section of Czech Astronomical Society holds a national conference on variable stars, stellar astrophysics in general and since recently also on extrasolar planets. In the last three years the conference took place in the public observatory of the city Valasske Mezirici, replacing the previous venue Brno.

Our conferences on variable star research provide unique opportunities for meetings between professional and amateur astronomers and have become a crucial platform for exchanging information and sharing knowledge. These events help to keep the local astronomical community alive and active.

This year's conference was held on a weekend from November 14 to November 17 and we celebrated its 40th anniversary. All participants were able to witness the richness of our field and the joy that research on variable stars brings to our lifes.

I would like to express gratitude to all authors for their talks and posters and to all participants for their contribution to the discussions!

Luboš Brát
- president of Variable Star and Exoplanet
Section of Czech Astronomical Society

Pec pod Sněžkou, November 17, 2008

OPEN EUROPEAN JOURNAL ON VARIABLE STARS
September 2009 http://var.astro.cz/oejv ISSN 1801-5964

A new HADS type variable star in Auriga

V.PŘIBÍK [1], L.BRÁT [2]

(1) Hinata-sou Observatory, tř.3.května 689, 763 02 Zlín, Czech Republic, vasa@mobil.cz
(2) ALTAN.Observatory, Velká Úpa 193, 542 21 Pec pod Sněžkou, Czech Republic, http://pod.snezkou.cz/altan

Abstract: A report on a new High Amplitude Delta Scuti variable star in the EP Auriga field is presented in this paper. The star is identified as GSC 02420-00093, USNO-A2.0 1200-04473131 or CzeV166 Aur [CzeV] (α(2000) = 6h12m13:90s; δ(2000) =+31° 48' 25.3"). Its mean magnitude had been estimated as 13.1 mag with maximal amplitudes 0.15 mag in I, 0.25 mag in R and 0.35 mag in V bands. At least three pulsation modes have been identified, with dominant period of 0.0711 d. This report has been updated since its presentation at the conference to reflect the new findings.

Abstrakt: V tomto článku je prezentována nová proměnná hvězda typu High Amplitude Delta Scuti, která byla objevena v poli EP Aurigae. Tato hvězda je identifikována jako GSC 02420-00093, USNO-A2.0 1200-04473131 nebo CzeV166 Aur [CzeV] (α(2000) = 6h12m13:90s; δ(2000) =+31° 48' 25.3"). Její střední magnituda byla odhadnuta na 13,1 mag a maximální amplituda na 0,15 mag v I, 0,25 mag v R a 0.35 mag ve V pásmech. Byly nalezeny alespoň tři pulzační mody, s hlavní periodou 0,0711 dne. Tento článek byl oproti prezentaci na konferenci aktualizován, aby byly zahrnuty nové poznatky.

Whilst observing EP Aurigae variable star, variations in the brightness of another star (21.5' distant) were noticed (using [C-Munipack] software). A rather peculiar light-curve, with fluctuations of both width and height of peaks, suggested a physical variable star with non-radial pulsation modes. Further observations proved this to be the case and the type was estimated to be High Amplitude Delta Scuti.
Since its discovery in November 2008, several observation sessions, under significantly changing conditions and using different instrument setups, have been performed. Because of these difficult conditions the data could not be processed properly and only a preliminary analysis has been done. Using [Peranso] analysis software (trial version) and its Lomb-Scargle method implementation, three pulsation modes have been clearly identified. The period ratios (f2/f1 = 0,774505; f3/f2 = 0,772378) are consistent with typical HADS stars [Berger 1979]. All the findings have been confirmed using different software and method ([Period04] and FFT).

	elements	amplitude*)
f1	0,07105196 * E + 2454758,4180	65 mmag
f2	0,05503008 * E + 2454758,4072	23 mmag
f3	0,04250400 * E + 2454758,4170	10 mmag

*) average amplitude of all used filter bands

Table 1: CzeV166 Aur pulsation mode elements

date	length	points	band	observer
2008-10-18	231 min	371	clear	VP
2008-10-21	274 min	451	clear	VP
2008-10-23	158 min	251	clear	VP
2008-10-23	306 min	74	I	LB
2008-10-23	310 min	74	R	LB
2008-10-23	310 min	75	V	LB
2008-11-01	278 min	188	R*	VP
2008-11-02	195 min	141	R*	VP
2008-11-03	217 min	193	R*	VP
2008-11-05	347 min	310	R*	VP
2008-12-23	68 min	61	R*	VP
2008-12-28	260 min	64	I	LB
2008-12-28	269 min	64	R	LB
2008-12-28	252 min	62	V	LB

date	length	points	band	observer
2008-12-30	203 min	50	I	LB
2008-12-30	206 min	50	R	LB
2008-12-30	207 min	49	V	LB
2009-01-03	262 min	243	B*	VP
2009-01-08	232 min	209	B*	VP
2009-01-10	242 min	198	B*	VP
2009-01-12	247 min	52	I	LB
2009-01-12	190 min	46	R	LB
2009-01-12	243 min	41	V	LB

R* and B* are astrophotographic filters (an RGB set)

Table 2: Observations of CzeV166 Aur (Observation log)

observer	telescope, mount	camera	filter set
VP	imager: 10" [SkyWatcher] Newton, EQ6 Pro guider: 4" [SkyWatcher] refractor	[MII] G2-1600 [MII] G1-0400	RGB photographic
LB	imager: 8" [Vixen] Maksutov-Cassegrain, EQ6 Pro guider: 80 mm [Celestron] refractor ED	[SBIG] ST-8 [MII] G1-2000	BVRI photometric

Table 3: Instruments used

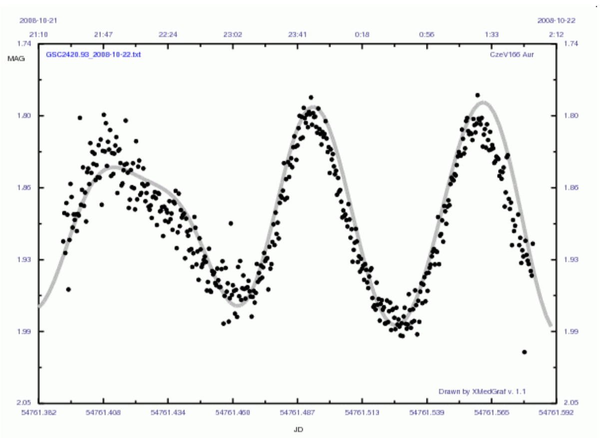

Figure 1: CzeV166 Aur, 2008-10-18, clear (unfiltered)

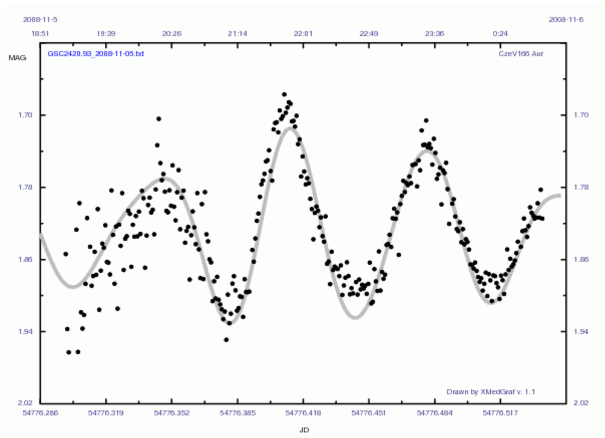

Figure 2: CzeV166 Aur, 2008-11-05, R* band

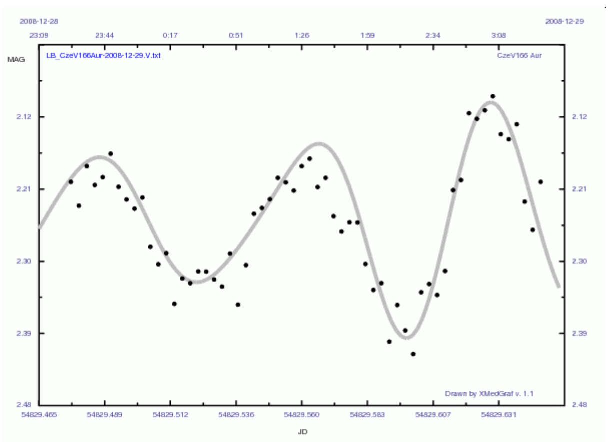

Figure 3: CzeV166 Aur, 2008-12-29, V band

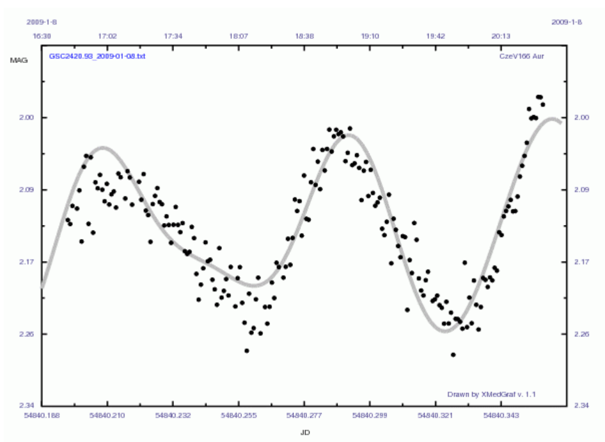

Figure 4: CzeV166 Aur, 2009-01-08, B* band

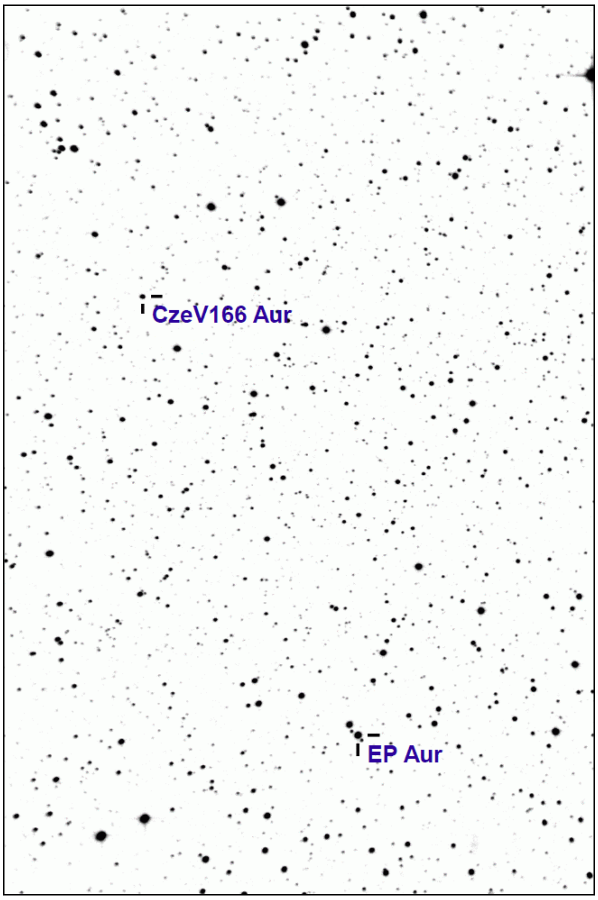

Figure 5: Identification map

Plans for further study:

The main obstacle to proper analysis of the data is the wide range of filters used (observations should be analyzed separately for every band). Therefore, longterm and regular observation with one or two filters only is needed and hopefully will be done. After the required data has been obtained, much more careful analysis will be performed and more-in-depth article published.

References

[CzeV] Suspected variable stars catalogue CzeV http://var.astro.cz/newvar.php

[Observation log] http://var2.astro.cz/EN/obslog.php?obs_id=1&star=CzeV166%20Aur

[C-Munipack] http://c-munipack.sourceforge.net/

[Peranso] http://www.peranso.com/

[Berger 1979] Berger, M., 1979, Delta Scuti and related stars (1979PASP...91....5B)

[Period04] http://www.univie.ac.at/tops/Period04/

[MII] http://ccd.mii.cz/

[SBIG] http://www.sbig.com/

[SkyWatcher] http://www.skywatchertelescope.net/

[Vixen] http://www.vixenoptics.com/

[Celestron] http://www.celestron.com/

OPEN EUROPEAN JOURNAL ON VARIABLE STARS
September 2009 http://var.astro.cz/oejv ISSN 1801-5964

Alternative methods for detection of GRBs

R. HUDEC[1], M. SPURNY[2], M. KRIZEK[3], P.PATA[4], R. SLOSIAR[5] AND M. RERABEK[4]

(1) Astronomical Institute, Academy of Sciences of the Czech Republic, 251 65 Ond¡rejov, Czech Republic, and Czech Technical University, Faculty of Electrical Engineering, Prague, Czech Republic
(2) Karlovy Vary Observatory, Karlovy Vary, Czech Republic
(3) Charles University, Prague, Czech Republic
(4) Czech Technical University, Faculty of Electrical Engineering, Prague, Czech Republic
(5) Partizanske Observatory, Amateur Astronomer, Bojnice, Slovak Republic

Abstract: We report on two altenative simple methos to detect counterparts of cosmic gamma-ray bursts (GRBs). We report on the development and tests of an alternative optical all-sky monitor recently tested at the Karlovy Vary Observatory. The monitor is based on a Peleng 8 mm .sh-eye lens (1:3,5-1:16) and CANON EOS 350D digital CCD camera. This type of monitor represents a low-cost device suitable for easy replication and still able to detect brighter optical transients simultaneously to GRB triggers. Such OTs have been observed for some of the GRBs such as GRB990123, GRB060117, or recently GRB0803 indicating that some fraction of GRBs can generate optical transient emission accessible by simple small aperture instrumentation as described here. These efforts are accompanied by development of dedicated programmes to access and to evaluate all-sky images, these efforts will be also brie.y described. The All-Sky Monitor is a space variant optical system and its point spread function (PSF) has not uniform shape in the .eld of view. The processing and measuring of image data is complicated and sophisticated deconvolution algorithms are used for image restoration. The second method is the GRB detection based on thein ionospheric response.

GRB detection by bright prompt optical emission GRB

Even the fastest optical follow-up telescopes cannot access the times close or identical to times of GRBs, and the time domain before GRB remains completely hidden.

These time domains can be accessed only by optical wide-.eld monitors (as the position of the GRB is unpre-dictable). The all-sky monitors offer the best sky coverage. An alternative approach is to monitor the FOVs of recent GRB satellites with optical WF cameras. Some of the all-sky monitors operated on daily basis are based on the use of photographic emulsion (allowing long exposures and .ne spatial resolution). However, the photographic emulsion is not very sensitive to short optical .ares and has some additional disadvantages.

The alternative digital all-sky monitoring is provided by the CONCAM system. However, the limiting magnitudes are not very deep, so one can hardly expect such system will be able to detect optical transients (OTs) of GRBs.

The brightest OTs related to GRBs observed so far were observed at magnitudes 6–10 (e.g. GRB990123, GRB060117, GRB080319) [1][3]. For GRB060117, the optical transient was followed due to technical reasons from 2 min after the GRB trigger and already declining, so one can deduce that the peak brightness probably exceeded mag 8 [2]. We hence need monitors able to detect short OTs with duration of about 1 min and fainter than magnitude 8.

The instrumentation

The used instrumentation is simple and low-cost. The camera has two parts, namely the Peleng 8 mm .sh-eye lens (1:3,5-1:16) that provides a 24 mm circular 180 ¡r .eld of view, and a CANON EOS 350D digital CCD camera. The total cost of the hardware is around 1500 USD, ie. one order less than the CONCAM system. One can hence expect the system to be easily and cheaply replicated to numerous sites. One can consider the alternative type of the digital camera, such as Canon EOS 5D with a larger CCD chip (but somewhat larger pixel size) hence covering the whole FOV of the .sh-eye lens. We plan to improve the performance of the system by designing, in collaboration with the Czech Technical University in Prague, specialy dedicated mount and miniature dome for the camera.

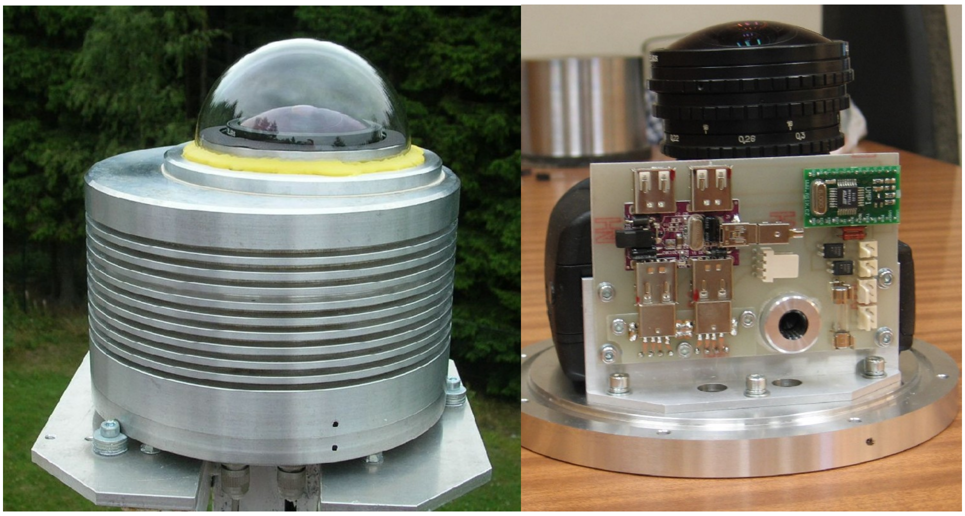

Figure 1: The assembled all–sky camera in observing conditions (left) and the camera with control electronic board (right)

Figure 2: An example of raw non-guided image, exposure time 80 sec

Simulation and evaluation of images from optical all-sky systems

There are two related problems in WFC and UWFC optical systems:(1) optical aberrations and (2) space variant systems The motivation for the simulation is as follows: (1) modeling of optical system used in all-sky monitors and their transfer characteristics aberrations and distortion (2) UPSF image restoration and deconvolution of acquired image data removal and (3) enhancement of measurement precision.

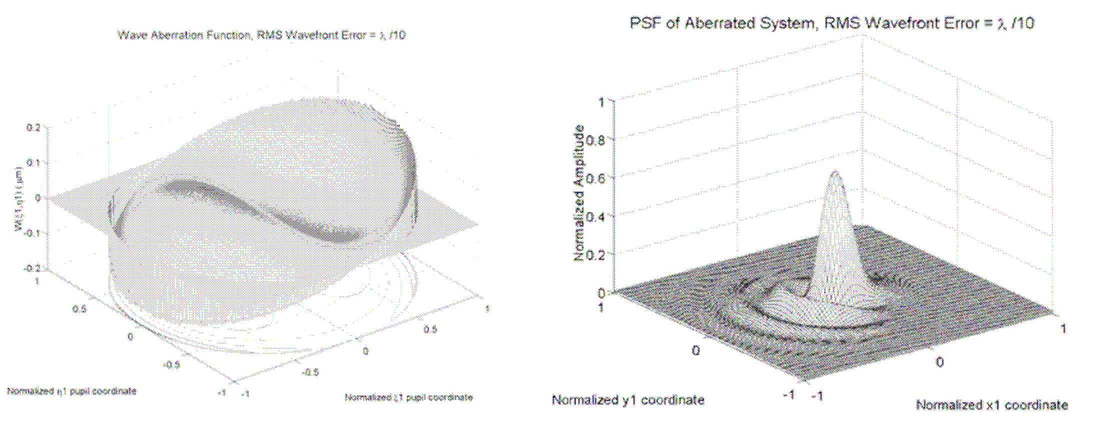

Figure 3: Examples of modelling of optical abberations in optical all-sky monitors

Real UWFC image data and their evaluation are related with the following problems: (1) objects on ultra wide-.eld images are very small (a few pixels per object dimension). (2) optical aberrations and distortions in UWFC systems (3) infuence of optical aberrations increases at the edges of FOV (4) these aberrations distort the PSF of optical system and rapidly cutthe accuracy of measurements. (5) objects on the frontier of .eld of view are not usedfor analysis inastrometry because a lot of aberrations.

The VLF detections of GRBs

The method of indirect detections of GRBs at VLF has been described already efore [1], however only very few positive records are known. Previously reported VLF detections of GRBs are as follows. (i) GRB830801. A first observation of an ionospheric disturbance from a gamma-ray burst reported [1]. The burst occurred at 22:14:18 UT on August 1, 1983, and was one of the strongest ever observed at that time. The total fluence was 0.002 erg/sq cm, most of which occurred in the .rst 4 s of the burst. Simultaneously, a change was observed in the amplitude of a VLF radio signal from a transmitter in Rugby, England indicative of an ionospheric disturbance. Weaker disturbances were also recorded at the same receiving site on sinals from VLF stations in Annapolis, Maryland and Lualualei, Hawaii. The times of the burst and the disturbances are coincident within the 10-s reso-lution of the VLF recording system. No similar disturbances were observed within 60 hr around the time of the burst. (ii) SGR1806: detection of a Sudden Ionospheric Disturbance [5], (iii) GRB030329 observed asaSudden Ionospheric Disturbance (SID) [6]. Although there were numerous e.orts to detect GRBs by VLF and despite the fact that the necessary instrumentation is inexpensive, this field still remains little exploited.

PHYSICS BEHIND IONOSPHERIC DETECTION

The solar particle stream, solar wind, shapes and controls the Earths magnetic envelope -the magnetosphere-and increases heat in the aurora zones. But not all ionospheric variability is caused by solar or geomagnetic disturbances. The ionosphere is not a constant 'mirror in the sky'. The E layer (100-200km aboveground) and the F1 layer (170-200km) usually behave in regular, solar–controlled way, but the F2 layer (250-350 km) does not. It is the F2 layer, which has the greatest density of free electrons, and is potentially the most efective reflector of radio waves [7].

The ionossperic D layer plays in the GRB detections an important role, as the detection of X-ray and gamma-ray triggers is based on the measurement (monitoring) of reflected radio waves from this layer. The ionospheric D layer is not transparent for radio VLF waves (frequencies 3kHz to 30kHz) and behaves like a mirror. If the transmitter is at large distance (800 to2000 km) then the radio waves are guided like in a waveguide consisting of the D layer and the earth surface. Any change in the quality of this waveguide results then in the signal change in the SID monitor. The change can be positive but in some cases such as the suddenphase anomaly also negative.

Recent VLF detections of GRBs

We present below examples of VLF/SID detection in three cases: GRB 060124A, GRB080319D and GRB080320A, as well as Hind for detection of GRB induced propagating ionospheric waves.

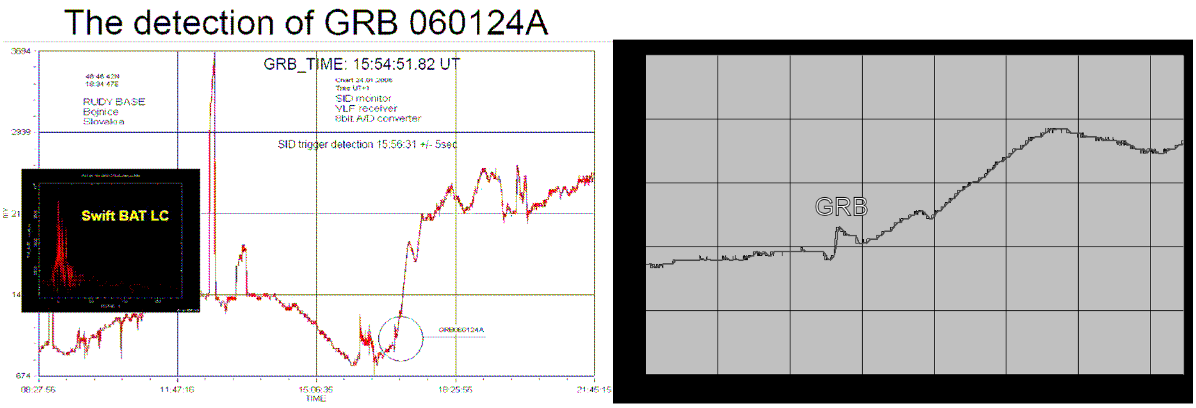

Figure 4: The detection of GRB 060124A

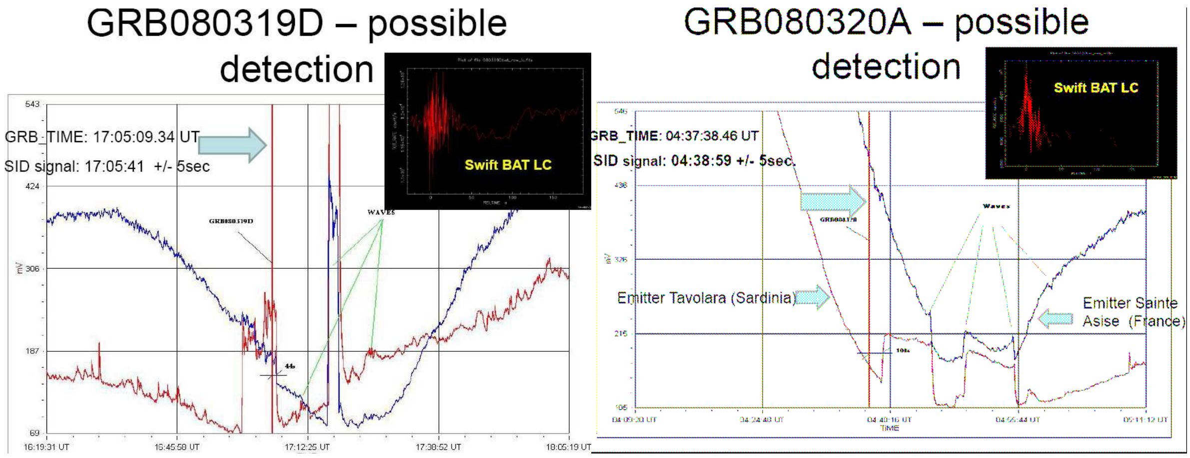

Figure 5: The probable detection of GRB080319D (left) and GRB080320A (right) with indicated probable propagating ionospheric waves caused by the GRB.

Conclusions

An alternative low-cost (~ 1.5 kUSD) optical digital all-sky monitoring system has been assembled and it is tested recently. The preliminary results indicate the limiting magnitude even for non-guided system and for one image with exposure of 30 sec amounts to mag 8. Deeper magnitudes are expected for guided system and longer or cumulated exposures, then the expected limiting magnitude can reach the mag 9–10 range. This makes the system suitable for wide-.eld monitoring in the sky for brighter optical transients. The system can be very easily duplicated to numerous sites. Future improvements are planned such as desing of a miniature camera mount and dome to allow guided images and development of dedicated control and evaluation software. The algorithms for evaluation of images from all-sky monitors were developed and tested.
The independent and indirect detection of GRBs by their ionospheric response (SID, Sudden Ionospheric Disturbance) observed at VLF (Very Low Frequency) is feasible. We presented and discussed examples of such VLF/SID detection in three cases: GRB 060124A, GRB080319D and GRB080320A. In addition, these

measurements are in agreement with the scenario of propagating ionospheric waves triggered by the relevant GRBs. Although few such detections have been already reported in the past,the capability of such alternative and indirect investigations of GRBs, as well as the possible contribution to analyses of GRBs, still remains to be investigated in more details.

Acknowledgments

The GRB analyses described here are linked to the GRB analyses within the ESA PECS INTEGRAL Project 98023. Some parts are related to the grant of the Grant Agency of the Czech Republic 205/08/1207. The analyses of GRBs in optical range are newly supported by MSMT KONTAKT Project ME09028.

References

[1] Akerlof, C. et al., Nature, Volume 398, Issue 6726, pp. 400-402 (1999).

[2] Jelinek M. et al., Astronomy and Astrophysics, Volume 454, Issue 3,L119-L122 (2006).

[3] Racusin, J. L. et al.,Nature, Volume 455, Issue 7210, pp. 183-188 (2008)

[4] Fishman, G. J.; Inan, U. S., Nature, 331, 418-420(1988).

[5] P. Campbellet al., GCN, 2932,(2003).

[6] P. W. Schnoor et al.,GCN, 2176,(2003).

[7] Rishbeth, H.; Mller-Wodarg, I. C. F.; Zou, L.; Fuller-Rowell, T. J.; Millward, G. H.; Mo.ett, R. J.; Idenden, D. W.; Aylward, A. D., Annales Geophysicae, 18, Issue 8, 945-956,(2000).

OPEN EUROPEAN JOURNAL ON VARIABLE STARS
September 2009 http://var.astro.cz/oejv ISSN 1801-5964

Brief demonstration of the new developed database of the transiting planets

STANISLAV PODDANÝ [1,2]

(1) Astronomical Institute, Charles University, V Holešovičkách 2, Prague, Czech Republic
(2) Štefánik observatory, Petřín 205, Prague 1, Czech Republic,
email: poddany@observatory.cz

Abstract: Exoplanet Transit Database (ETD) consists from three individual sections. One is for predictions of the transits, second for processing new light curves to the database and the last section includes the O-C diagrams of the derived values from each light curve - the central transit time, duration and the depth of the transit.

Abstrakt: Databáze tranzitujících exoplanet (ETD) se skládá ze tří částí. Předpovědi tranzitů, dále části sloužící k nahrávání nových pozorování a tzv. O-C brány, kde jsou vykreslovány určené hodnoty tranzitu – okamžik středu tranzitu, jeho hloubka a délka trvání.

Introduction

Exoplanet Transit Database (ETD) came into existence in September 2008 as a project maintained by the Variable Star and Exoplanet Section of Czech Astronomical Society. This database was originally projected as an O-C gate for amateur exoplanet observes collected in the project TRESCA[1]. ETD was designed to be a web application because of this we developed fast, reliable and reasonably precise semiautomatic procedure for uploading and processing the light curve to the database.

Demonstration of the database

Commonly used methods for determination the mid-eclipse time in the case of eclipsing binaries (such a Kwee and van Woerden (1956) method) aren't possible to use in the case of transiting planets. The light curves of the exoplanet transits usually have very short ingress and egress parts and the signal-to-noise ratio is usually small. In spite of this fact many amateur observes use this methods for determination the mid-transit time of their light curves.

Because of this in the section *"Model fit data"* of the ETD we developed fast, reliable and reasonably precise code that is based on the Mandel&Agol (2002) model of the exoplanet transit. This model we simplified using the linear darkening law with the fixed value of the coefficient ($c_1 = 0.5$), farther we take over impact parameter and other values of the parameters from literature. As a fitting procedure we used the Levenberg-Marquardt non-linear least squares algorithm from Press et al. (1992). These simplifications allowed us to get the results of the transit mid-time, duration and the transit depth in the fraction of the second. The results including the errors are plotted in the section of the *"O-C gate"*. Each exoplanet have its own plot of the mid-transit time, depth of the transit and the transit duration (Figure 1).

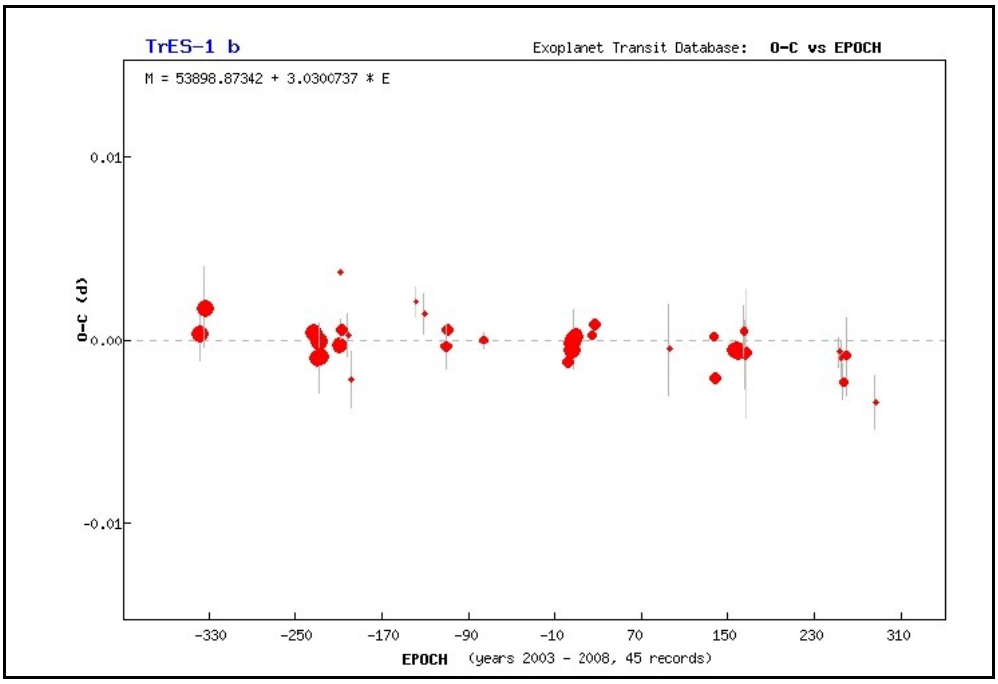

Figure 1: Transit central time O-C plot for the exoplanet TrES-1 b.

Each observer can also find the prediction of the transits for the next month in the section *"Transit prediction"* for any place all over the world (Figure 2). Except predictable time of the transit beginning/center/end, duration and the depth of each transit are there also displayed the location of the object on the sky.

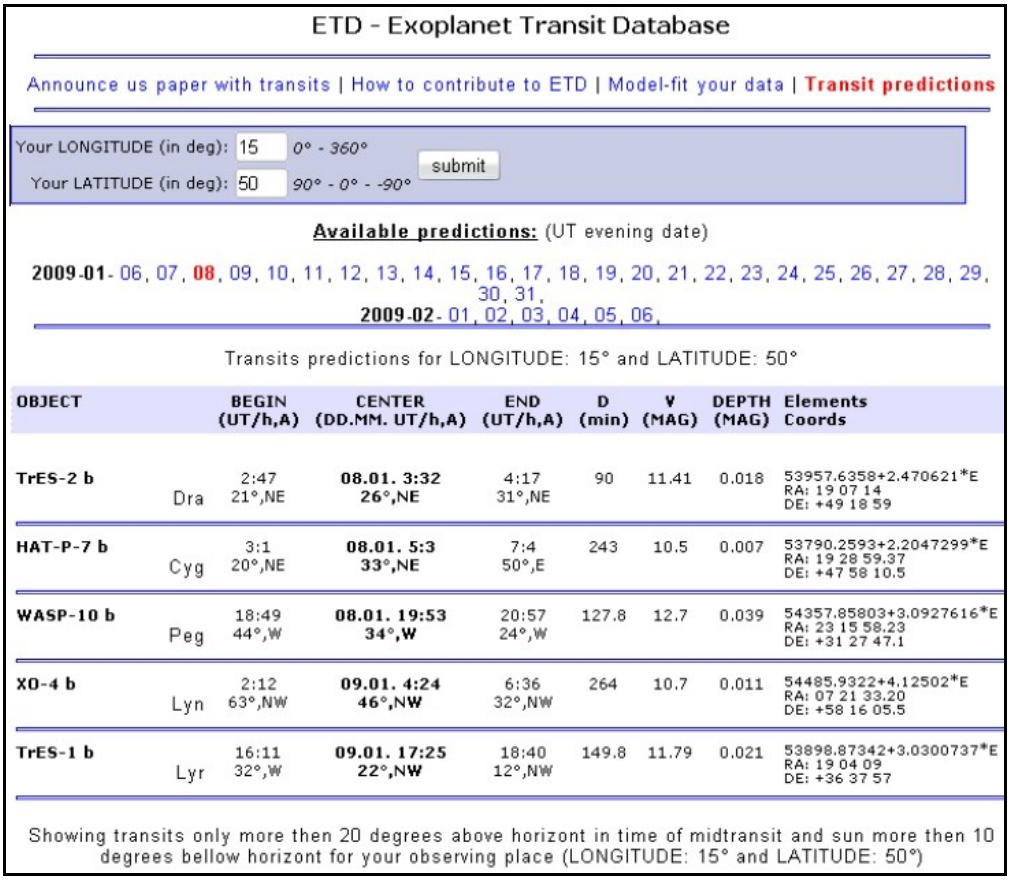

ETD - Exoplanet Transit Database

Announce us paper with transits | How to contribute to ETD | Model-fit your data | Transit predictions

Your LONGITUDE (in deg): 15 0° - 360°
Your LATITUDE (in deg): 50 90° - 0° - -90°
submit

Available predictions: (UT evening date)

2009-01- 06, 07, 08, 09, 10, 11, 12, 13, 14, 15, 16, 17, 18, 19, 20, 21, 22, 23, 24, 25, 26, 27, 28, 29, 30, 31,
2009-02- 01, 02, 03, 04, 05, 06,

Transits predictions for LONGITUDE: 15° and LATITUDE: 50°

OBJECT		BEGIN (UT/h,A)	CENTER (DD.MM. UT/h,A)	END (UT/h,A)	D (min)	V (MAG)	DEPTH (MAG)	Elements Coords
TrES-2 b	Dra	2:47 21°,NE	08.01. 3:32 26°,NE	4:17 31°,NE	90	11.41	0.018	53957.6358+2.470621*E RA: 19 07 14 DE: +49 18 59
HAT-P-7 b	Cyg	3:1 20°,NE	08.01. 5:3 33°,NE	7:4 50°,E	243	10.5	0.007	53790.2593+2.2047299*E RA: 19 28 59.37 DE: +47 58 10.5
WASP-10 b	Peg	18:49 44°,W	08.01. 19:53 34°,W	20:57 24°,W	127.8	12.7	0.039	54357.85803+3.0927616*E RA: 23 15 58.23 DE: +31 27 47.1
XO-4 b	Lyn	2:12 63°,NW	09.01. 4:24 46°,NW	6:36 32°,NW	264	10.7	0.011	54485.9322+4.12502*E RA: 07 21 33.20 DE: +58 16 05.5
TrES-1 b	Lyr	16:11 32°,W	09.01. 17:25 22°,NW	18:40 12°,NW	149.8	11.79	0.021	53898.87342+3.0300737*E RA: 19 04 09 DE: +36 37 57

Showing transits only more then 20 degrees above horizont in time of midtransit and sun more then 10 degrees bellow horizont for your observing place (LONGITUDE: 15° and LATITUDE: 50°)

Figure 2: Transit prediction window

Discussion

Soon after the initiation became the ETD very popular among the observers. We started to take over all available light curves (amateur and professional). After one month of the existence of the ETD we have more than 400 light curves into the database. In the future we would like to improve the quality distribution of the light curves (now the light curves are divided into 5 groups according the "eye quality filter").

Acknowledgements

We thank the Czech Astronomical Society for the web hosting and general maintenance of this project. This investigation was supported by the Grant Agency of the Czech Republic, grant No. 205/08/H005. We also acknowledge the support from the Research Program MSM0021620860 of the Ministry of Education.

References

[1] TRESCA project http://var2.astro.cz/EN/

Mandel K., Agol E., 2002, ApJ, 580, 171

Kwee, K. K., van Woerden, H. 1956, Bull. of the Astr. Inst. of the Netherlands, 464, 327

Press W. H., Teukolsky S. A., et al., 1992, Cambridge: University Press, 1992, Numerical recipes in C. The art of scientific computing

OPEN EUROPEAN JOURNAL ON VARIABLE STARS
September 2009 http://var.astro.cz/oejv ISSN 1801-5964

Can we find other bodies in transiting extrasolar systems?

MARIE HRUDKOVÁ[1]

(1) Astronomical Institute of the Charles University, Faculty of Mathematics and Physics, Prague, Czech Republic, mariehrudkova@gmail.com

Abstract: Searching for transit timing variations in the known transiting exoplanet systems can reveal the presence of other bodies in the system. Here I discuss the current state of such an effort and the chances for a finding any transit timing variations from both ground and space-based observations.

Abstrakt: Hledání změn předpokládaných dob středů primárních zákrytů tranzitujících extrasolárních systémů může odhalit přítomnost dalších těles přítomných v systému. Zde diskutuji o současném stavu a případných šancích na úspěch nalezení nějakých změn z pozemských a vesmírných pozorování.

Introduction

Ground-based radial velocity and photometric transit surveys have been the most successful methods for discovering planets over the past decade with a yield of more than 300 extrasolar planets discovered to date. The most of so far detected planets are of Jupiter mass, whereas the planets of Earth-mass regime are still to be found. However, there is still a chance to discover planets similar to the Earth from measurements of transit timing variations (TTVs) in known transiting planetary systems (Agol et al. (2005), Holman & Murray (2005)).
If there is another planet in the transiting system the motion of a transiting planet is perturbed and the period of mid-eclipses shows variations. To be able to see any variations one needs to determine the time of mid-eclipse with a sufficient accuracy, and this can be obtained only from a good quality photometry. Then one needs to observe at least several transits to confirm any TTVs which could result in discovering other bodies in the system or at least placing limits on their existence. In the mid-eclipse times of transits of transiting exoplanetary systems one can find either short-term variations that could reveal the presence of moons, trojans or other planets (Holman & Murray (2005), Agol et al. (2005) and Ford & Holman (2007)), or long-term variations that could result from orbital precession (Miralda-Escudé (2002)). Finding such variations would provide further constraints on theories of planetary system formation and evolution, as well on theories of planetary atmospheres and their composition.

The data accuracy

As was already mentioned, for TTVs analyses one needs to measure mid-transit times with a sufficient accuracy. The higher the accuracy, the stronger the limits on other bodies in the system. Unfortunately, there can be many effects cutting down the accuracy of the measurements. In ground-based observations determination of transit times can be affected by systematic errors arising from the Earth's atmosphere or imperfections of the optics and the instrument used for observations. Moreover, the achievable accuracy limit for ground-based observations is imposed by scintillation and is around 1 mmag. Therefore it is highly desirable to search for TTVs from space observations.
Another important issue in determining accurate transit times is the importance of having a light-curve that is well-sampled during both ingress and egress, because the transit timing is most sensitive at these parts. If either ingress or egress is missing, the transit is only partial and there is a bigger chance of getting large systematic errors in the transit timing determination.

TTVs modelling:

The summary of techniques that can be used for TTVs analyses is following. The simplest approach is using direct N-body integrations of a large sample of planetary systems in order to directly fit the observed TTV signal (Holman & Murray (2005), Agol et al. (2005)). However, this method is extremely CPU expensive because of the large number of unknown parameters. Recently, Nesvorný & Morbidelli (2008) proposed an analytic perturbation theory method which is much faster than direct N-body integrations. Currently the method is not suitable when mean motion resonances between the two planets occur but they give an alternative solution to this problem.

Discoveries:

From ground-based observations so far a clear TTVs evidence was published by Díaz et al. (2008) for OGLE-TR-111 transiting system, suggesting a presence of a planet with the mass of the Earth in an exterior orbit if the orbit of OGLE-TR-111b is eccentric, which is not ruled out by the current radial velocity data. Other TTVs evidence was found by Welsh (2009) for HD 17156 transiting system suggesting the presence of a third body. Using space observations strong limits on the presence of other bodies for HD 209458 (Miller-Ricci et al. (2008a)), HD 189733 (Croll et al. (2007), Miller-Ricci et al. (2008b)) and CoRoT-Exo-2 (Alonso et al. (2008)) transiting systems were placed. In a near future accurate long-time series of transiting extrasolar planets suitable for TTVs analyses will be granted by CoRoT and Kepler space missions.

References:

Agol, E., Steffen, J., Sari, R., & Clarkson, W. 2005, MNRAS, 359, 567

Alonso, R., Aigrain, S., Pont, F., Mazeh, T. 2008, IAU Symposium n. 253 Proceedings, in press

Croll, B., Matthews, J. M., Rowe, J. F. et al. 2007, ApJ, 671, 2129

Díaz, R. F., Rojo, P., Melita, M. et al. 2008, ApJ, 682, L49

Ford, E. B., & Holman, M. J. 2007, ApJ, 664, 51

Holman, M. J., & Murray, N. W. 2005, Sci, 307, 1288

Miller-Ricci, E., Rowe, J. F., Sasselov, D. et al. 2008, ApJ, 682, 586

Miller-Ricci, E., Rowe, J. F., Sasselov, D. et al. 2008, ApJ, 682, 593

Miralda-Escudé, J. 2002, ApJ, 564, 1019

Nesvorný, D., & Morbidelli, A. 2008, ApJ, 688, 636

Welsh, W. F. 2009, AAS Meeting 213, 319.01

OPEN EUROPEAN JOURNAL ON VARIABLE STARS
September 2009 http://var.astro.cz/oejv ISSN 1801-5964

ESA Gaia: The variability based on low dispersion spectra

RENÉ HUDEC, VOJTĚCH ŠIMON, LUKÁŠ HUDEC, MATÚŠ KOCKA & COLLABORATORS & GAIA CU7 CONSORTIUM

Group of High Energy Astrophysics, Stellar Department,Astronomical Institute of Academy of Sciences of the Czech Republic, Ondřejov, Czech Republic
ISDC Versoix, Switzerland
Czech Technical University in Prague, Faculty of Electrical Engineering, Prague, Czech Republic

Abstract: The ESA satellite in development Gaia to be launched in 2011 will focus on highly precise astrometry of stars and all objects down to limiting magnitude 20. Albeit focusing on astrometry related matters, the satellite will also provide photometric and spectral information and hence important inputs for various branches of astrophysics. Within the Gaia Variability Unit CU7 and related work package Specific Object Studies there has been a sub-work package accepted for optical counterparts to celestial high-energy sources, a category which includes the optical counterparts (i.e. optical transients and optical afterglows, including counterparts of XRFs and yet hypothetical orphan afterglows) of GRBs, and also microquasars. Although the sampling of photometric data will not be optimal for this type of work, the strength of Gaia in such analyses is the .fine spectral resolution (spectro-photometry) which will allow the correct classication of related triggers. The possibilities to detect and to analyze optical transients and optical afterglows of GRBs and microquasars by Gaia will be presented and discussed, as well as variability studies based on low-dispersion spectra for selected categories of objects.

Introduction

Gaia is a cornerstone astrophysical mission of the European Space Agency ESA, see http://astro.estec.esa.nl for more details. It is a global space astrometry mission (Perryman, 2005). Its goal is to make the largest, most precise map of our Galaxy by surveying an unprecedented number of stars. Gaia is a mission that will conduct a census of billions stars in our Galaxy. It will monitor each of its target sources about 100 times over a .ve-year period. It is expected to discover hundreds of thousands of new celestial objects, such as extra-solar planets and failed stars called brown dwarfs. Within our own Solar System, Gaia should also identify tens of thousands of asteroids. Gaia will measure the positions, distances, space motions, and many physical characteristics of some one billion stars in our Galaxy and beyond.
It is obvious that, with the above briefy described performance, the Gaia will provide valuable inputs to various research .elds of contemporaneous astronomy and astrophysics including the .eld of high-energy sources. Most of the variable object research will be performed within the Gaia Variability Coordination Unit CU7. To study the optical counterparts of celestial high-energy sources, there will be several advantages provided by Gaia. First, this will be a deep limiting magnitude of 20 (Jordi and Carrasco, 2007), much deeper than most of previous studies and global surveys. For example, no detailed statistics of variable stars has been investigated for magnitudes fainter than 18. Secondly, the time period covered by Gaia observations, i.e. 5 years, will also allow some studies requiring long-term monitoring, recently provided mostly by astronomical plate archives and small or magnitude-limited sky CCD surveys. But perhaps the most important bene.t of Gaia for these studies will surely be the color (spectral) resolution thanks to the low resolution (prism) Gaia spectroscope. This will allow some detailed studies involving analysis of color and spectral changes not possible before. Another valuable input will come from the parallax measurements – the knowledge of directly measured distances of the sources will be highly bene.cial. The details of studies of the optical counterparts of high-energy sources have been recently evaluated and are described in more detail mostly by the dedicated sub-workpackages within the workpackage Speci.c objects studies within the Gaia CU7 (Hudec et al., 2007a, Hudec et al., 2007b).
The main objective of the sub–workpackage mentioned above is the investigation and analysis of optical counterparts of high-energy astrophysical sources (including High-Mass X-Ray Binaries, Low-Mass X-Ray Binaries, X-Ray Transients, X-Ray Novae, Optical Transients and Optical Afterglows related to X-Ray Flashes and Gamma-Ray Bursts, Microquasars etc.) based on the Gaia data as complex analysis with additional data.

The Spectral Power of Gaia

The Gaia telescopes offer unique variability studies based on low-dispersion spectra, i.e. the energy resolution of recorded star images (as these are represented by prism low–dispersion spectra). In this context, the application of algorithms developed for digitized astronomical archival plates (Hudec L., 2007) may be important for Gaia (see Figure 1 showing example of simulated Gaia prism spectra and of digitized astronomical Schmidt plate prism spectra). The novel algorithms for automated analysis of digitized spectral plates have been recently developed by informatics students (Hudec L., 2007) and are suitable for (1) Automated classi.cation of spectral classes, (2) Searches for spectral variability (both continuum and lines), (3) Searches for objects with specific spectra, (4) Correlation of spectral and light changes, and (5) Searches for transients.

Gaia and GRBs

A relatively large fraction of Optical Afterglows (OAs) of GRBs is within the Gaia limit on mag 19 hence their fading light curves will be obtained with high accuracy. However, the sampling provided by Gaia, is not optimal for goals of detection of new OAs of GRBs, hence not always we can expect realiable and confirmed detection of OAs of GRBs based only on photometry by Gaia

The primary strength of Gaia for OAs study is the fine spectro-photometry and low-dispersion spectroscopy. This can give additional, so far little exploited additional input to the study and investigation of OAs, and perhaps even to help search for and to verify yet hypothetical orphan afterglows of GRBs.

The OAs of GRBs are known to exhibit speci.c colors and this can be used to detect OAs of GRBs based on detailed color information. Fine division of the light signal into a number of .lters in the Gaia instrument will provide us with information on the spectral energy distribution and color indices of very faint objects. Among others, observing the optical afterglows (OAs) of GRBs and the associated supernovae, which appear in the .eld of view during the Gaia scans, will be possible. The speci.c color indices of these objects (Figure 3) [9, 10, 11] and their time evolution will be very helpful in this regard. This method will enable also a searching for the so-called orphan afterglows, i.e. GRBs from which no gamma-ray emission is observed because of an unfavorable direction of the beam with respect to the observer. Since the optical emission is less beamed, it can be still observed, as predicted by theory [8]. The specific color indices of the optical afterglows of long GRBs (Figure 3) can be very helpful in resolving the orphan afterglows from other kinds of object.

The Three Observing Modes of Gaia

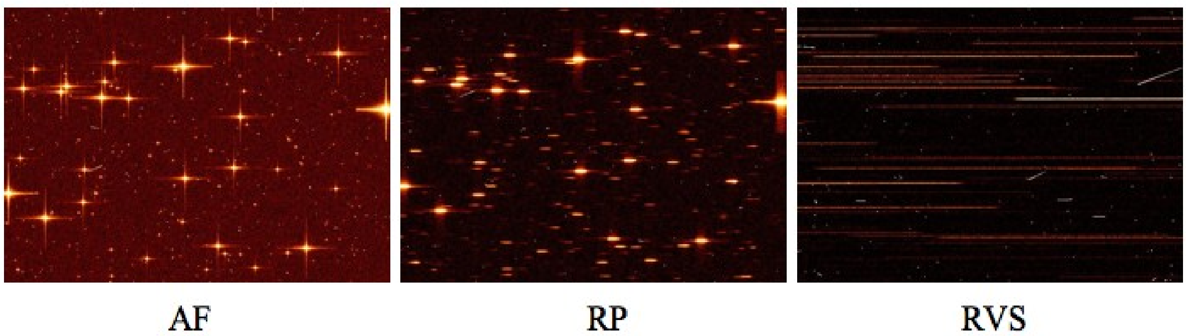

Figure 1: The three observation modes: AF = astrometric, RP = photometric, RVS = spectrophotometric.

In this paper we focus of the „photometric mode“ RP/BP. In reality this mode generates ultra low-dispersion prism spectra.

The use of dispersive element (prisma) generates ultra low-dispersion spectra. One disperser called BP for Blue Photometer operates in the wavelength range 330-660 nm; the other called RP for Red Photometer covers the wavelength range 650-1000 nm. The dispersion is higher at short wavelengths, and ranges from 4 to 32 nm/pixel for BP and from 7 to 15 nm/pixel for RP.

Simulated Gaia low dispersion spectra

Gaia's photometric instrument is based on a dispersive-prism approach such that starlight is not focused in a PSF-like spot but dispersed along the scan direction in a low-resolution spectrum.

The instrument consists of two low-resolution fused-silica prisms dispersing all the light entering the FOV. One disperser called BP for Blue Photometer operates in the wavelength range 330-660 nm; the other called RP for Red Photometer covers the wavelength range 650-1000 nm. Two CCD strips are dedicated to photometry, one for BP and one for RP. Both strips cover the full astrometric FOV in the across-scan direction.

All BP and RP CCDs are operated in TDI (time-delayed integration) mode. The CCDs have 4500 (for BP) or 2900 (for RP) TDI lines and 1966 pixel columns (10 x 30 micron pixels).

The spectral resolution is a function of wavelength as a result of the natural dispersion curve of fused silica. The dispersion is higher at short wavelengths, and ranges from 4 to 32 nm/pixel for BP and from 7 to 15 nm/pixel for RP. The BP and RP dispersers have been designed in such a way that BP and RP spectra have similar sizes (on the order of 30 pixels along scan).

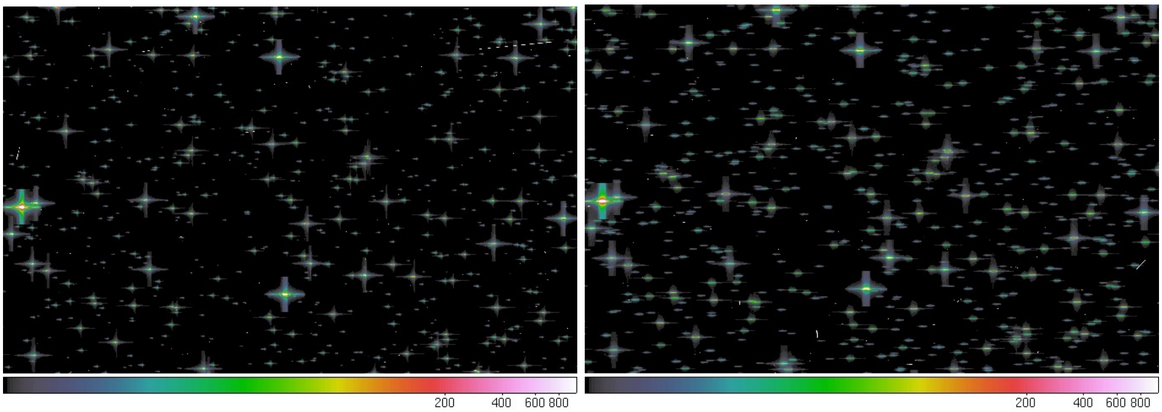

Figure 2: Simulated by GIBIS simulator BP (left) and BR (right) images, the same sky field.

BP and RP spectra will be binned on-chip in the across-scan direction; no along-scan binning is foreseen. RP and BP will be able to reach object densities on the sky of at least 750,000 objects deg-2. The obtained images can be simulated by the GIBIS simulator (see Figure 2).

Why a Variability Study based on low dispersion spectra is important

Some astrophysical objects exhibit relation of spectral and photometric variations, for example Mira Variables. For example, the Mira variable X Cam (T. Jarzebowski, 1959) is known to exhibit spectral variations M0 to M6.5, accompanied by photometric variations with amplitude 1.4 mag in R (Figure 3)..

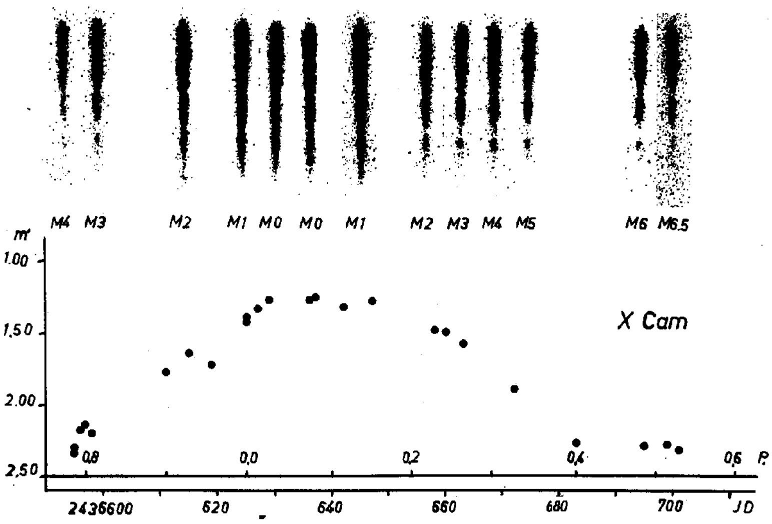

Figure 3: Spectral and photometric variability of X Cam (T. Jarzebowski, 1959).

The Cepheid Variables represent another example. All classical Cepheids definitely vary their spectral types. At maximum, they all have types around F5-F8. At minimum, the longer the period, thelater is the spectral type (to K2) (Samus, 2008).
Examples of related spectral and photometric variations of Cepheids were shown e.g. by Becker, F. 1938, and Shapley 1916.
Spectral type changes of peculiar stars are also known: For example, the variable FG Sagittae changed its spectral type from B to M (Chalonge et al 1977).

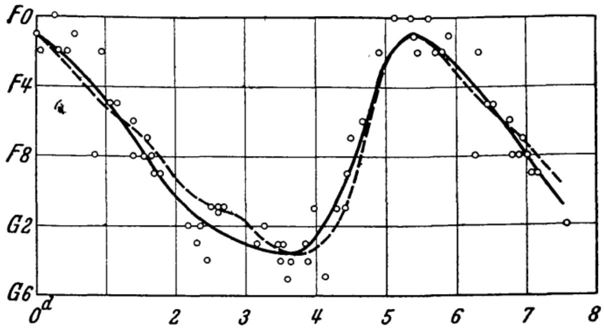

Abb. 1. Mittlere Spektralkurve und visuelle Lichtkurve (gestrichelt) von δ Cephei.

Figure 4: Relation of photometry and spectral type for delta Cephei (Becker 1938).

The Spectral Type Variability with Gaia

- It is known that certain types of variable stars (VS) such as Miras, Cepheids, and peculiar VS exhibit large variations in their spectral types
- This fields is however little exploited, as before were these studies very laborious (plates were mostly visually inspected) and limited. No review on spectral variability among VS exists (Samus, personal comm. 2008)
- The evaluation by computers and dedicated s/w will allow to search and investigate spectral variability in Gaia data and in digitized Spectral plates

Suitable Low Dispersion Spectral Databases for Gaia

Before Gaia, low dispersion spectra were frequently taken in last century by various photographic telescopes with objektive prisma. Some of them are listed below.

- Sonneberg Schmidt Camera
- Sonneberg Bolivia Expedition: Southern Sky Coverage
- Hamburg Quasar Spectral Survey
- Digitised Byurakan Spectral Survey

Schmidt Camera Sonneberg

The dispersion ~ 23 nm/mm at Hg for the 3 deg prisma. The scan resolution is 0.05 mm/px, thus about 0.5 nm/px. The dispersion ~ 10 nm/mm at Hg for the 7 deg prisma. The scan resolution is 0.02 mm/px, thus about 0.2 nm/px.

Bolivia Expedition Spectral Plates

Coverage of Southern Sky with Spectral and Direct Plates. Potsdam Observatory, plates stored at Sonneberg Observatory. Hidden for ~75 years. Plates taken ~ 1924-1928, about 70 000 prism spectra estimated and published in Potsdam Publ. 26-19 in 1930.

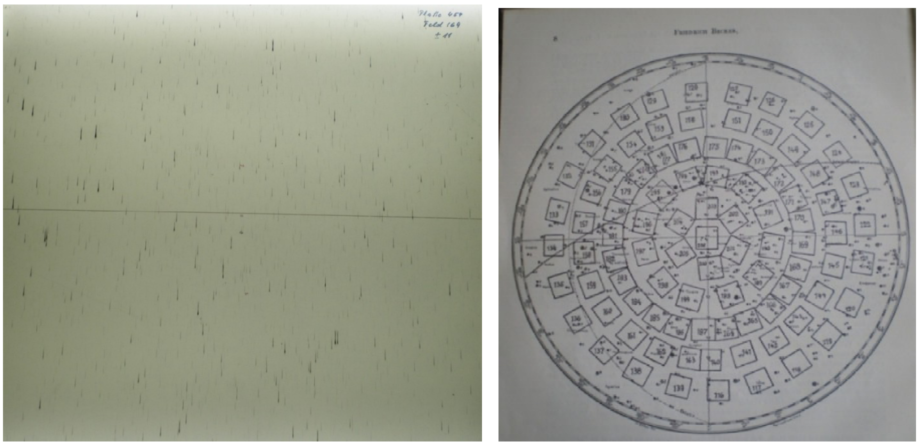

Figure 5: Bolivia Expedition spectral plates (left) and southern sky coverage of Bolivia Expedition spectral plates (right).

Hamburg Quasar Survey

Discovery objective prism spectrum of HS0822+3542, emision line galaxy. The wavelength coverage is 3200A (upper end) to 5400A (lower end). HS0822+3542 shows almost nothing but the O[III] 5007A emission line (the black dot) is seen, while the continuum is barely visible.
A wide-angle objective prism survey searching for quasars with B<17.5 on the northern sky. The survey plates have been taken with the former Hamburg Schmidt telescope, which is located at Calar Alto/Spain since 1980. For the survey the 1.7°prism was used providing unwidened objective prism spectra with a dispersion of 139 nm/mm at Hgamma. Under conditions of good seeing the FWHM of the images is 30 µm (plate resolution) giving a spectral resolution of 4.5 nm at Hgamma on the objective-prism plates. Online access.

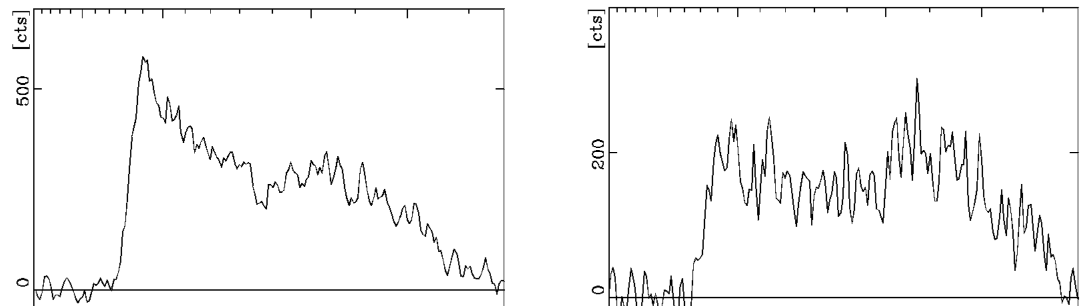

Figure 6: Example spectra of cataclysmic variable (left) & blazar (right, digitised Hamburg Survey)

Byurakan Survey

The Digitized First Byurakan Survey (DFBS) is the digitized version of the First ByurakanSurvey (FBS). It is the largest spectroscopic database in the world, providing low-dispersion spectra for 20,000,000 objects on1139 FBS fields = 17,056 deg2 Online access. Sky coverage: DEC>-15°, all RA (exceptthe Milky Way). Prisma spectral plates by 1 m Schmidt telescope. Limiting magnitude: 17.5 in V. Spectral range: 340 –690 nm, spectral resolution 5 nm. Dispersion: 180 nm/mm near H-gamma.

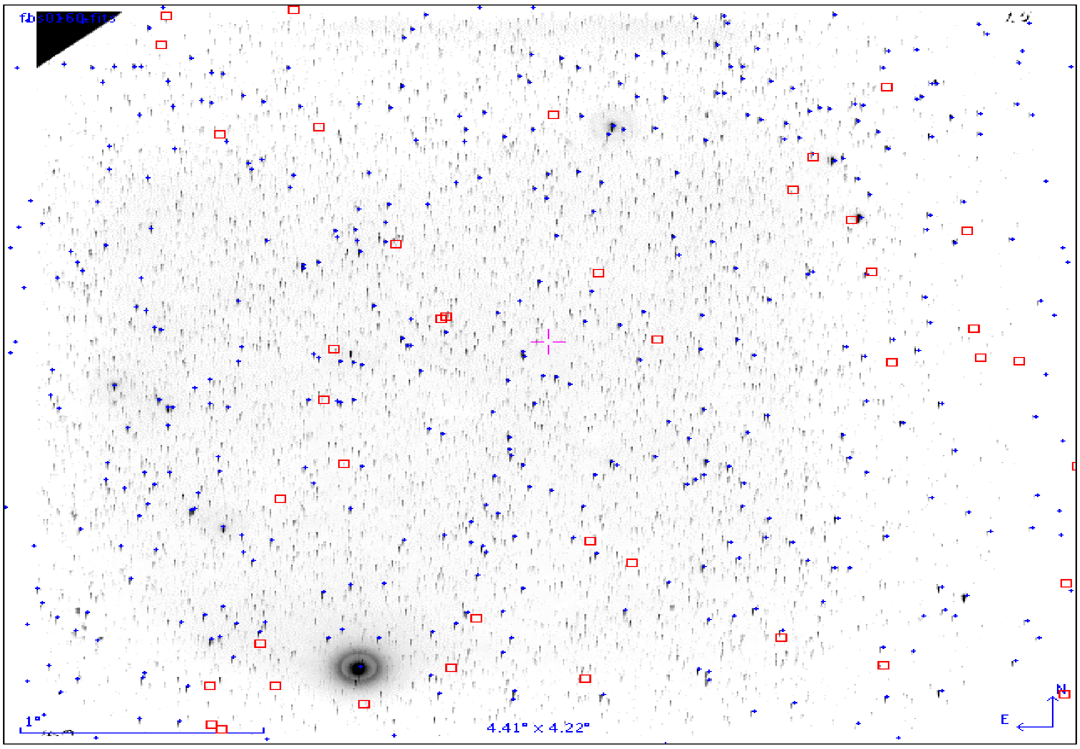

Figure 7: An example of Byurakan Spectral Plate (FOV = 4°x4°)

Algorithms for automated analyses of digitized spectral plates

- Developed by informatics students
- Automated classification of spectral classes
- Searches for spectral variability (both continuum and lines)
- Searches for objects with specific spectra
- Correlation of spectral and light changes
- Searches for transients
- Application for Gaia expected

The Motivation

- The archival spectral plates taken with objective prisma offer the possibility to simulate the Gaia low dispersion spectra and related procedures such as searches for spectral variability and variability analyses based on spectro-photometry

- Focus on sets of spectral plates of the same sky region covering long time intervals with good sampling –simulating the Gaia BP/RP outputs

Automatic classification of stellar objective prism spectra on digitised plates, a simulationand afeasibilty study for low-dispersion Gaia spectra

The Ultra Low Dispersion Spectral Images by Gaia

Why Ultra-Low: RP and BP will be able to reach object densities on the sky of at least 750,000 objects deg-2.

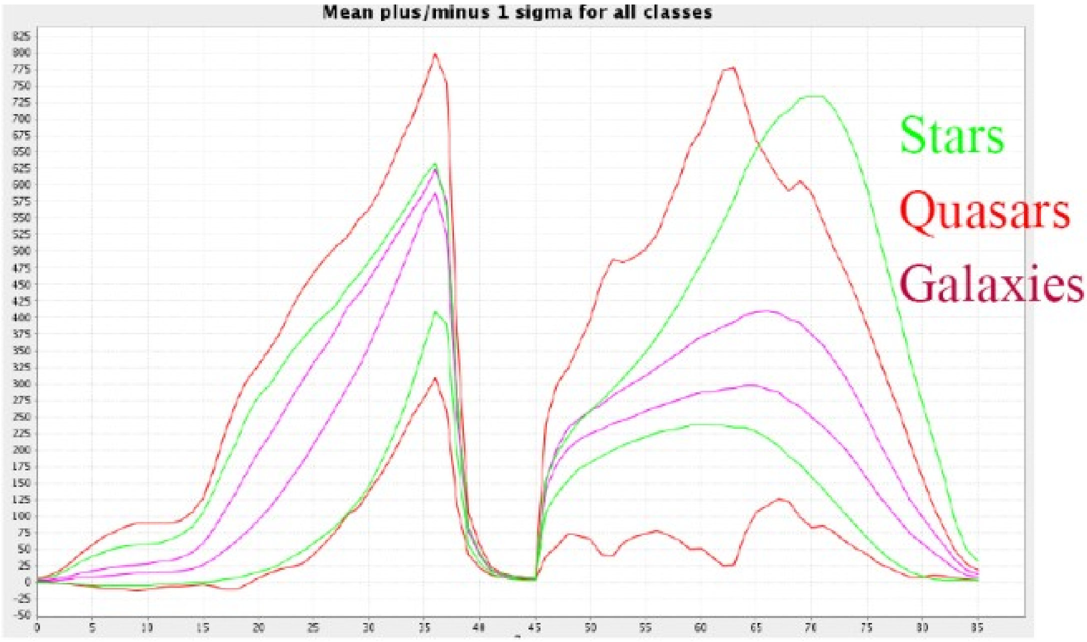

Figure 8: The simulated 1D Low Disp Spectra by Gaia according to Bailer-Jones et al., 2008

Examples of objects with very strong spectral lines expected to be accessible by Gaia BP/RP are given below.

Planetary Nebulae

Spectrum of planetary nebula NGC 7009 (Saturn Nebula). In the upper left corner the positioning of the slit is indicated. The low-resolution spectra is shown as both a graph and an emission line profile. The high resolution spectrum is shown in the upper right centered around the H line showing the presence of N+lines straddling the H line. Various other ionic and atomic species are identified. Many of these lines are forbidden such as the intense 5007 Angstrom line of O+2.

WR Stars Type WC

Wolf-Rayet star HD 165763 (type WC). Notice the distinguishing feature of these stars, the emission lines of multi-ionized states of Carbon and Oxygen. The wavelength range spans from 3420A at the upper left to 9730A in the lower right.

WR Stars Type WN

Wolf-Rayet star HD 190918 (type WN) associated with NGC 6888, the Crescent Nebula. Note the strong, broad lines of ionized Nitrogen and Helium in emission, typical of these type stars.

Comparison Gaia Low Dispersion Spectra Versus Spectral Plates

The Dispersion

- Gaia BP: 4-32 nm/pixel i.e. 400-3200 nm/mm, 9 nm/pixel i.e. 900 nm/mm at Hg, RP: 7-15 nm/pixel i.e. 700-1500 nm/mm. PSF FWHM ~ 2 px i.e. spectral resolution is ~ 18 nm.
- Plates Schmidt Sonneberg (typical mean value): the dispersion for the 7 deg prisma 10 nm/mm at Hg, and 23 nm/mm at Hg for the 3 deg prisma.The scan resolution is 0.02 mm/px, thus about 0.2 and 0.5 nm/px, respectively.
- Bolivia Expedition: 9 nm/mm, with calibration spectrum

- Hamburg QSO Survey: 1.7 deg prisma, 139 nm/mm at Hg, spectral resolution of 4.5 nm at Hg
- Byurakan Survey: 1.5 deg prisma, 180 nm/mm at Hg, resolution 5 nm at Hg
- Hence Gaia BP/RP dispersion ~ 5 to 10 times less than typical digitised spectral prism plate, and spectral resolution ~ 3 to 4 times less. Note that for plates the spectral resolution is seeing limited hence the values represent best values. Gaia BP/RP dispersion ~ 5 to 10 times less than typical digitised spectral prism plate, and spectral resolution ~ 3 to 4 times less, but on plates affected by bad seeing only ~ 2 times less.

	Wavelength range, nm	Limiting magnitude	Dispersion at Hg nm/mm	Spectral resolution nm
Gaia	330-660, 650-1000	~19	900	~18?
Sonneberg Schmidt	340-650	18	10 and 23	~3
Bolivia Expedition	340-650	14	9	~3
Hamburg	340-540	19	139	4.5
Byurakan	340-690	17.5	180	5

Table 1: Comparison of parameters of Gaia BR and BP and of selected plate low dispersion spectra

The motivation of these studies is as follows.

- Comparing simulated Gaia BP/RP images with those obtained from digitised Schmidt spectral plates (both using dispersive elements) for 8 selected test fields
- Feasibility study for application for algorithms developed for plates for Gaia

Very Preliminary Results

- Simulated Gaia BP/RP images affected by image distorsion, need for deconvolution
- In general 2D image quality worse than obtained from Schmidt plates
- Ultra low dispersion for Gaia, and hence limited use of spectra
- No lines detectable in BP/BR test images so far
- Study of continuum possible but still affected by image distorsions
- Not clear whether the suggested dispersion is optimal one!

Discussion

- The BP and RP will provide ultra low-dispersion spectra representing fully new and challenging task for astrophysicists and informatics as never used before
- Nearest analogy are low dispersion spectral surveys with plates
- The final and real appearance of BP/RP images/spectra still not very clear: GIBIS simulator yields different results than given in various papers
- Operation of GIBIS simulator still not very user friendly with space for improvement
- We propose to construct and to run ground based simulator generating REAL 2D spectra images (camera with the same dispersion and pixelsize), as independent device as various predictions/simulations give different results

The power of Gaia spectro-photometry for science

Despite of low dispersion discussed before, the major strength of Gaia for many scientific fields will be the fine spectrophotometry, as the low dispersion spectra may be transferred to numerous well defined color filters

Gaia and GRBs: Spectroscopy

- The primary strength of Gaia for GRB study is the fine spectro-photometry
- The OAs of GRBs are known to exhibit quite typice colors, distiguishing them from other types of astrophysical objels (Simon et al.2001,2004)
- Hence a realiable classification of OTs will be possible using this method

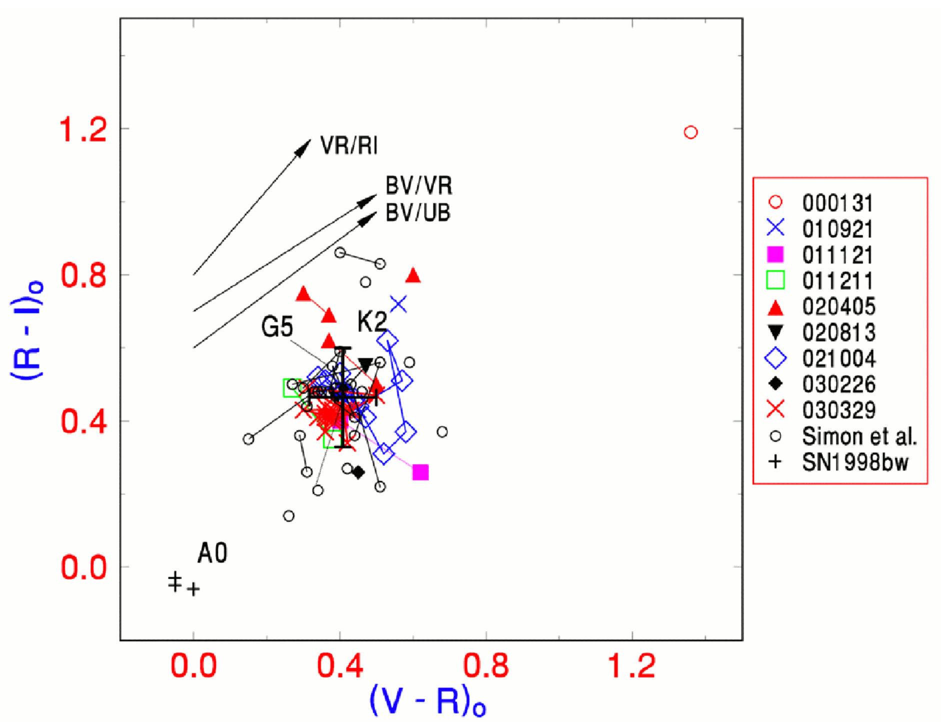

Figure. 9: V-R vs. R-I diagram of OAs of GRBs (t-T0<10.2 days) in observer frame, corrected for the Galactic reddening. Multiple indices of the same OA are connected by lines for convenience. The mean colors (centroid) of the whole ensemble of OAs (except for GRB000131) are marked by the large cross. The colors of SN1998bw are shown only for comparison. The representative reddening paths for EB-V=0.5 are also shown. Positions of the main-sequence stars are included only for comparison. For more details on specific colors of OAs of GRBs see Simon et al. (2001, 2004). Notice the prominent clustering of colors and negligible color evolution during decline.

Colors of Microquasars

This color-color diagram contains the microquasars of various types:

- system with the optical emission dominated by the high-mass donor–CygX-1
- persistent systems with the optical emission dominated by the steady-state accretion disk–SS433, ScoX-1
- transient low-mass systems in outburst with the optical emission dominated by the accretion disk–GROJ1655-40, XTEJ1118+480 (the disk is close to steady-state in outburst)
- high-mass system CI Cam on the decline from its1999 outburst to quiescence

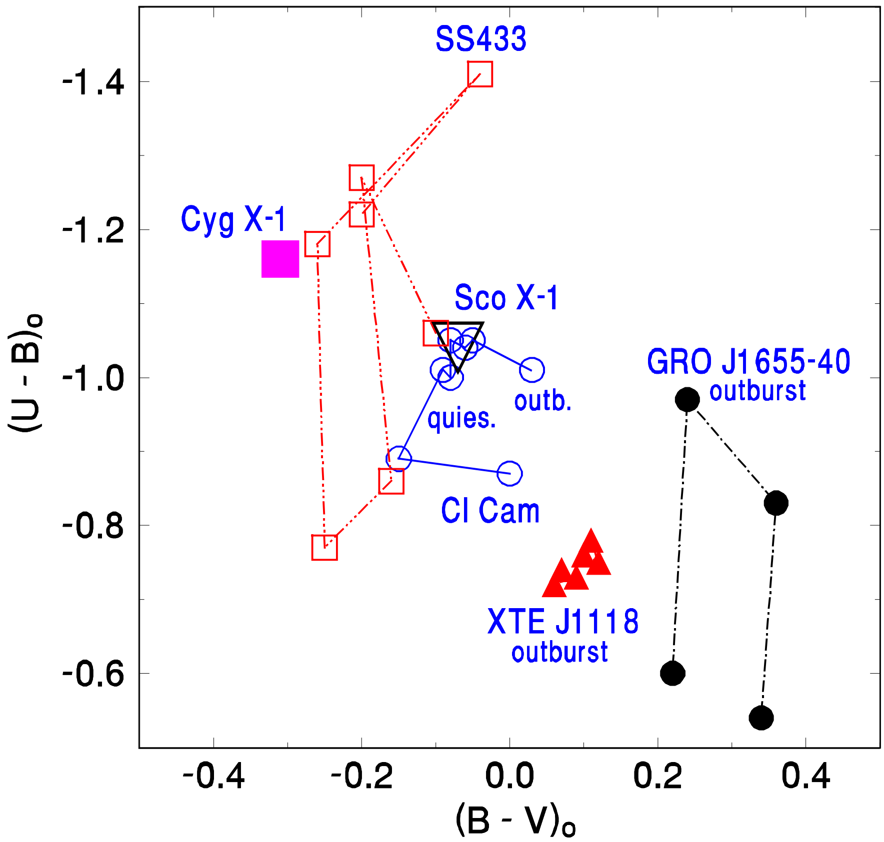

Figure 10: The color-color diagram for microquasars.

The systems plotted, irrespective of their types, display blue colors, with a trend of a diagonál formed by the individual objects.This method can be used even for the optically faint, and hence distant objects.

Conclusions

Gaia will provide ultra-low dispersion spectra by BP and RP representing a new challenge for astrophysicists and informatics.
The nearest analogy is represented by digitized prisma spectral plates: Sonneberg, Hamburg and Byurakan surveys
These digitised surveys can be used for simulation and tests of Gaia algorithms and Gaia data. Some algorithms have been tested already.
Some types of variable stars are known to exhibit large spectral type changes –this field is however little exploited and more discoveries can be expected with Gaia data as Gaia will allows to investigate spectral behaviors of huge amounts of objects over 5 years with (for spectroscopy) good sampling.

Acknowledgment

The Czech participation in the ESA Gaia project is supported by the PECS project 98058. The scientific part of the study is related to the grant 205/08/1207 provided by the Grant Agency of the Czech Republic. Some aspects of the project described here represent a natural continuation of the Czech participation to the ESA INTEGRAL (ESA PECS 98023). The analyses of digitised low dispersion spectral plates are newly supported by MSMT KONTAKT Project ME09027.

References

[1] Perryman, M. A. C., 2005, in Astrometry in the Age of the Next Generation of Large Telescopes, ASP Conference Series, Vol. 338, Proceedings of a meeting held 18-20 October 2004 at Lowell Observatory, Flagstaff, Arizona, USA. Edited by P. Kenneth Seidelmann and Alice K. B. Monet. San Francisco: Astronomical Society of the Paci.c, p.3

[2] Jordi, C. and Carrasco, J. M., 2007, in The Future of Photometric, Spectrophotometric and Polarimetric Standardization, ASP Conference Series, Vol. 364, Proceedings of a conference held 8-11 May, 2006 in Blankenberge, Belgium. Edited by C. Sterken. San Francisco: Astronomical Society of the Paci.c, p.215

[3] Hudec R. and Wenzel W., 1976, BAC, 27, 325.

[4] Hudec R., 1981, BAC, 32, 108.

[5] Hudec R., Simon V., 2007a, Speci.c object studies for cataclysmic variables and related objects ESA Gaia Reference Code GAIA-C7-TN-AIO-RH-001-1.

[6] Hudec R., Simon V., 2007b, Speci.c object studies for optical counterparts of high energy sources. ESA Gaia Reference Code GAIA-C7-TN-AIO-RH-002-1.

[7] Hudec L., 2007, Algorithms for spectral classi.cation of stars, BSc. Thesis, Charles University, Prague.

[8] Rhoads, J.E., ApJ, 487, L1 (1997).

[9] Šimon, V., Hudec, R., Pizzichini, G., and Masetti, N., A&A, 377, 450 (2001).

[10] Šimon, V., Hudec, R., Pizzichini, G., and Masetti, N., "Colors of Optical Afterglows of GRBs and Their Time Evolution," in Gamma-Ray Bursts: 30 Years of Discovery: Gamma-Ray Burst Symposium, edited by E. E. Fenimore and M. Galassi, AIP Conference Proceedings 727, American Institute of Physics, New York, 2004, pp. 487–490.

[11] Šimon, V., Hudec, R., and Pizzichini, G., A&A, 427, 901 (2004).

[12] http://sci.esa.int/gaia/

OPEN EUROPEAN JOURNAL ON VARIABLE STARS
September 2009 http://var.astro.cz/oejv ISSN 1801-5964

Photometry of extrasolar planets

TEREZA KREJČOVÁ[1]

(1) Department of theoretical physics and astrophysics, Faculty of science, Masaryk University, Brno

Abstract: This article is focused on the photometry of transiting extrasolar planets and on the determination of the star and exoplanet parameters from the light curve.

Abstrakt: Tento příspěvek se zabývá fotometrií tranzitujících extrasolárních planet a následným určením parametrů exoplanetárního systému z naměřené světelné křivky.

Transiting extrasolar planets

Extrasolar planets are nowadays quite fast expanding field of astronomy. Exploring these objects help us to understand the formation and evolution processes of stars and planetary systems. One of the most important group of exoplanets are the one with a unique orientation of their orbits with respect to the Earth - the so called transiting extrasolar planets. The whole geometry of the system is oriented in such a way, that the planet passes during its orbit across the parent star disk. As a consequence of this process we can photometrically observe a dip in an incoming flux of the star (see Figure 1) and in combination with the spectroscopical observations we can determine all of the most important parameters of the system.

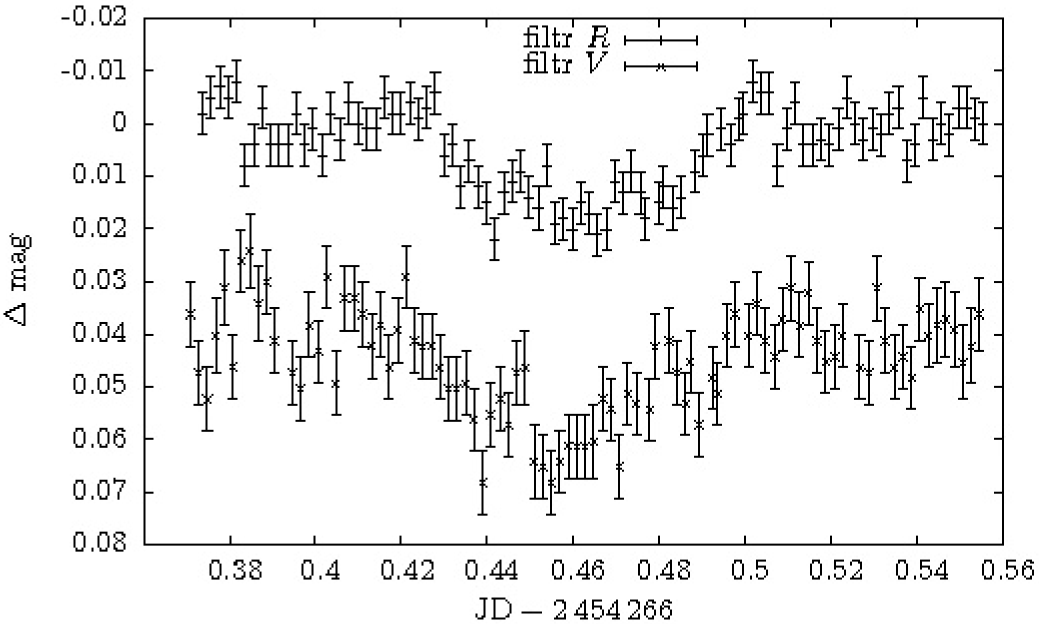

Figure 1: Light curve of exoplanetary transit of TrES-2 in filter R (Top) and in filter V (Bottom) from 14./15.6.2007. It was made by 62cm telescope at Masaryk university observatory.)

Determination of system parameters

There are two assumption I made:

We know the parameters of the parent's star (especially the radius and mass) and the planet's orbit is circular. Directly from the transit light curve we can determine four parameters: the middle of the eclipse, the duration of the eclipse t_Z, the duration of the central part of transit t_C and the depth of the transit ΔF. See Figure 2.

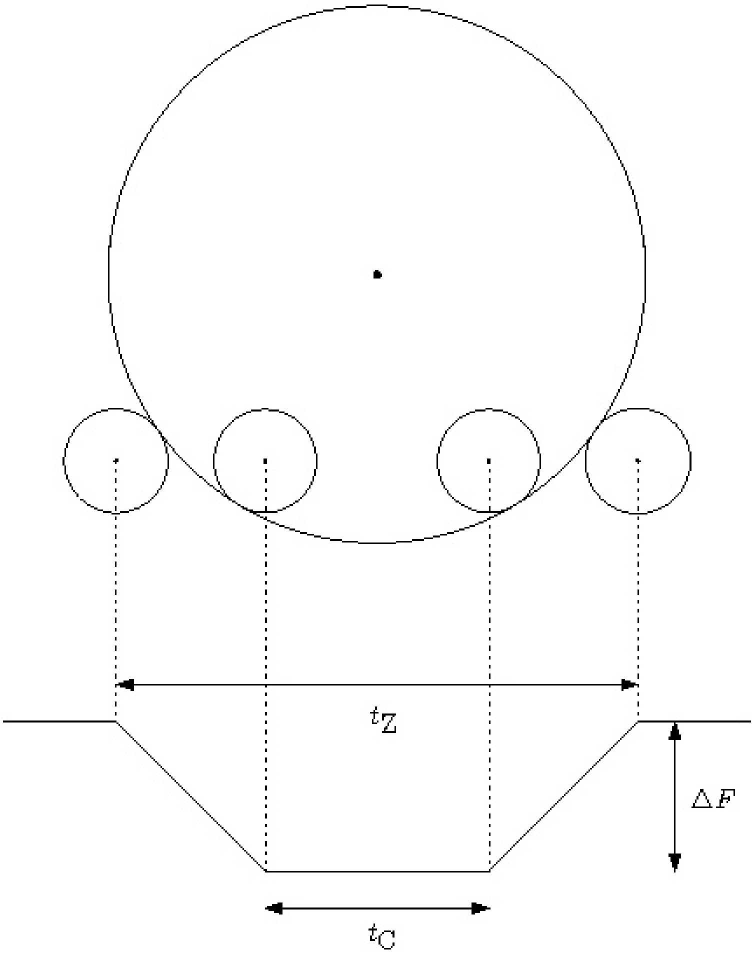

Figure 2: Parameters of transit

For determination of the middle of the eclipse and the duration of the eclipse I used AVE (www.astrogea.org). This programme was originally destined for finding the minima of eclipsing binary stars. To determine the orbital period of the exoplanet, more than one transit light curve is needed. The are two sources of data and transit light curves. The first one is Exoplanet Transit Database - ETD (http://var2.astro.cz/ETD/) and the latter is Amateur Exoplanet Archive - AXA (http://www.brucegary.net/AXA/x.htm).
If we know the parameters mentioned above we can due to the system geometry determine the radius of the exoplanet:

$$\Delta F = \left(\frac{R_P}{R_*}\right)^2,$$

where ΔF is the depth of the transit, R_* is the radius of the star and R_P is the radius of the planet.
The semi-major axis a could be calculated from the third Kepler's law, where we suppose the $M_P << M_*$:

$$a = \sqrt[3]{\frac{P^2 G M_*}{4\pi}},$$

where P is the orbital period, a is semi-major axis, G is the gravitational constant and M_* is the mass of the star.
The last parameter is inclination i:

$$i = \arccos\sqrt{\frac{(R_* + R_P)^2}{a^2} - \sin^2\frac{\pi t_Z}{P}},$$

where t_Z is the duration of the elipse. The parameters obtained for system TrES-2 using the above mentioned procedure are as follows:

TrES – 2		
Parameters	**Already published**	**Own calculations**
a [AU]	0.036 7 ± 0.0012	0.036 6 ± 1.3 · 10^{-3}
i [◦]	83.9 ± 0.2	84.2 ± 0.3
P [days]	2.470 63 ± 1·10^{-5}	2.470 63 ± 2.1 ·10^{-5}
R_P [R_J]	1.24 ± 0.09	1.20 ± 0.21
ΔF	–	0.015 ± 0.005
t_Z [days]	–	0.079 ± 0.002

Table 1: Parameters of extrasolar planet TrES - 2. a – semi-major axis, i – inklination, P – orbital period of the planet, M_P - mass of the planet, R_P – radius of the planet, ΔF – the depth of the transit, t_Z - time duration of the transit, R_J – radius of Jupiter. Published parameters were adopt from Donovan et al. (2006); Sozzetti et al. (2007).

Models of light curves

The parameters of system can be used for calculation of the theoretical light curves. The geometric model is based on the calculation of the area A(t) of the stellar disk eclipsed by the planet during the transit.

$$A(t) = 2\int_{\max(0,d(t)-R_P)}^{\min(R_*,d(t)+R_P)} r_* \arccos\gamma(t) dr_* \quad ,$$

where

$$\gamma = \frac{d^2(t) + r_*^3 - R_P^2}{2r_* d(t)}$$

for

$$r_* > R_P + d(t)$$

and

$$\gamma = -1$$

for the other cases. All the parameters are depicted in the Figure 3.

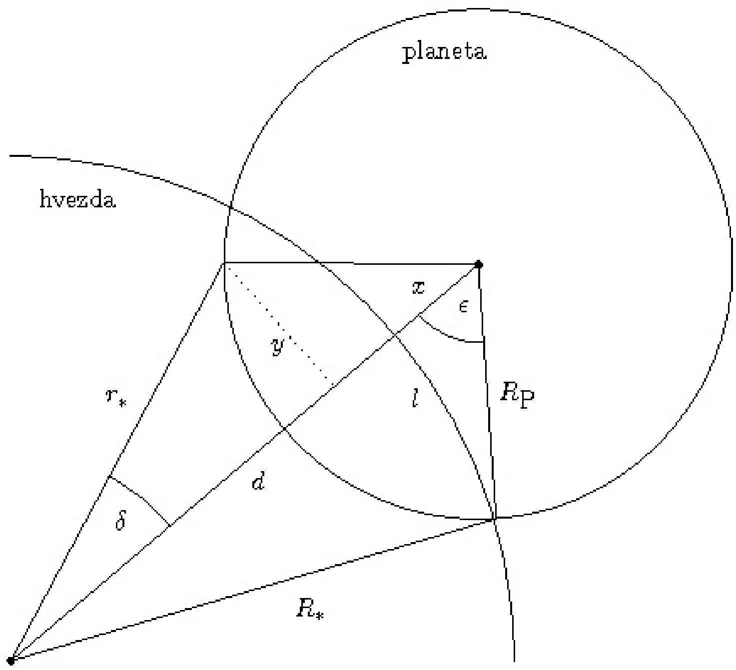

Figure 3: Model of transiting planet

The resulting shape of the light curve is given by the expression:

$$F(t) = 1 - \frac{A(t)}{\pi R_*^2}.$$

In the Figure 4 are model light curves for three values of radius of exoplanet.

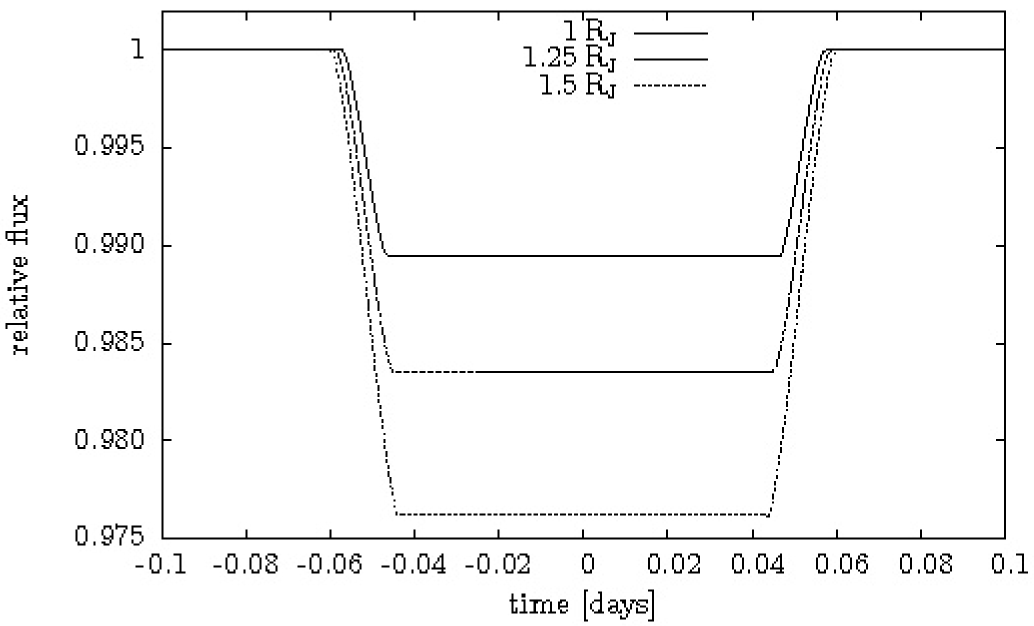

Figure 4: The shape of the light curve for three values of radius of exoplanet: 1, 1.5, 2 R_J. The other parameters of the system are a=0.05 AU, P = 3.5 days, $R_* = R_\odot$ and i = 90°).

We obtain more realistic model if we involve in it the limb darkening of the star. One possibility is the logaritmic law of limb darkening (vanHamme 1993):

$$I(\mu) = I(0)[1 - c_1(1-\mu) - c_2 \mu \ln \mu]$$

where I(μ) is the intensity on the disk at place mi, I(0) is the intensity in the middle of the disk, c_1,c_2 are the coefficients of limb darkening and $\mu = \sqrt{1 - \left(\frac{r_*}{R_*}\right)^2}$.

The shape of the curve is given by expression (Sackett 1999):

$$F(t) = 1 - \frac{\int_{\max(0, d(t) - R_P)}^{\min(R_*, d(t) + R_P)} r_* I(r_*) \arccos \gamma(t) dr_*}{\pi \int_0^{R_*} r_* I(r_*) dr_*}$$

,

The resulting light curve has slightly different shape from the previous one. See Figure 5.

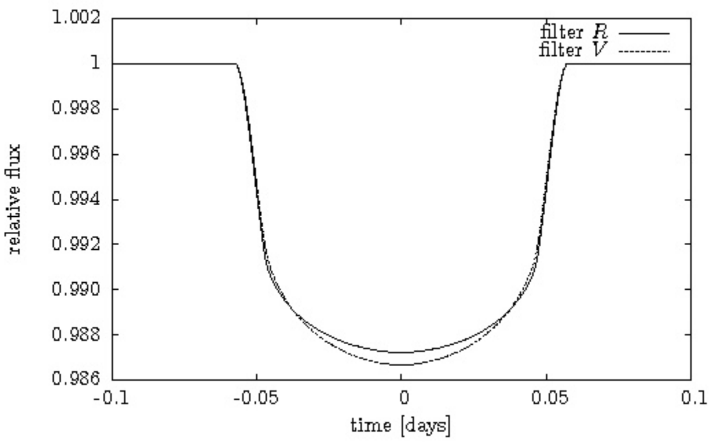

Figure 5: the model of the light curve of transiting extrasolar planet. The parameters of the star and planet: R_P = 1 RJ , a = 0.05 AU, i = 90° , P = 3.5 days, $R_* = R_\odot$, log g = 2.5 a Teff = 5 770 K.)

In the last picture, there are real data of TrES-2 with the fit based on the computed parameters of the system.

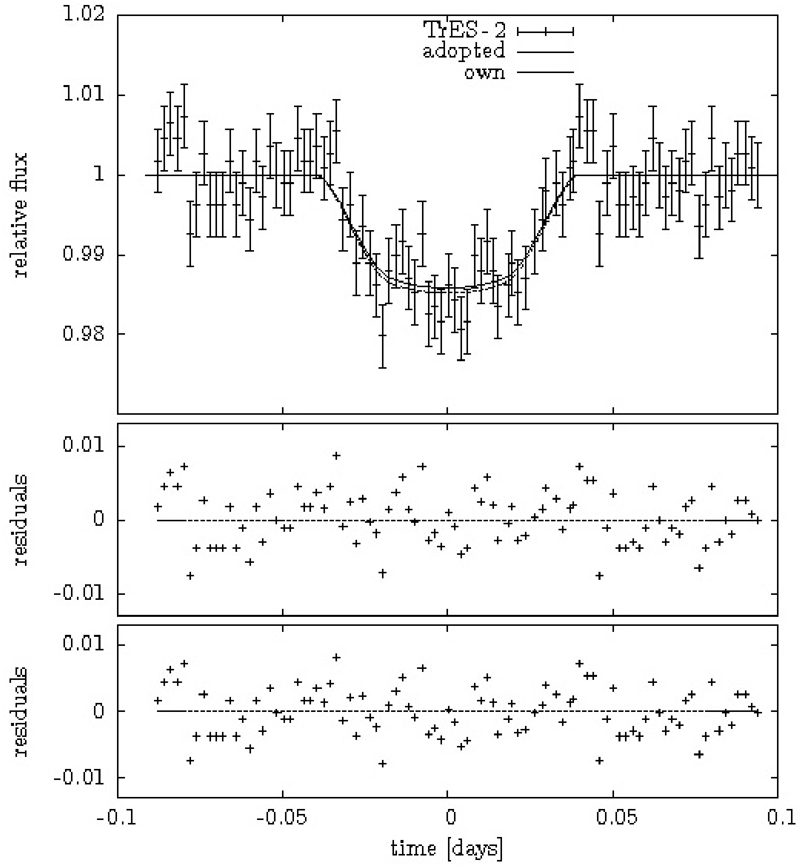

Figure 6: Top: Measured light curve of TrES-2 fitted by theoretical light curve. The solid line stands for the model based on parameters determined from the observed data. The dashed line stands for the model based on the parameters determined from the data presented in the scientific journals. Middle, bottom: data-model residuals for the solid, dashed line case.)

References

Cassen, P., Guillot, T., Quirrenbach, A. 2006, Saas-Fee Advanced Course 31:Extrasolar planets

O'Donovan, F.T., Charbonneau, D., Mandushev, G., et al. 2006, ApJ, 651, L61

Sozzetti, A., Torres, G., Charbonneau, D., et al. 2007, ApJ, 664, 1190

Sackett, P. D. 1999, in NATO ASIC Proc. 532, 189

Seager, S., Mallén-Ornelas, G., 2003, ApJ, 585, 1038

van Hamme, W. 1993, AJ, 106, 2096

http://www.astrogea.org/soft/ave/aveint.htm

http://var.astro.cz/

SID monitor indirect observation and monitoring of Solar flares

RUDOLF SLOSIAR[1]

(1) Rudy BASE (Bojnice Amareur Space Ear), Bojnice, Slovakia, Partizanske Observatory, rudy@8mag.net

Abstract: I introduce the method of indirect observation and monitoring of Solar flares. This reflex method is based on measuring of intensity of reflected radio wave from remote transmitter, which is working on VLF (very low frequency). Reflecting surface is created by ionosphere, so every change in its quality induced by Solar flare or by other cosmic event can be measured and thereafter evaluated as SID (sudden ionospheric disturbance).

Introduction

I introduce the method of indirect observation and monitoring of Solar flares. This reflex method is based on measuring of intensity of reflected radio wave from remote transmitter, which is working on VLF (very low frequency). Reflecting surface is created by ionosphere, so every change in its quality induced by Solar flare or by other cosmic event can be measured and thereafter evaluated as SID (sudden ionospheric disturbance).

Reflecting surface

For this Method, as reflecting surface we serve ionosphere, more accurately D layers of ionosphere. It is 100% dependent on direct solar radiation, therefore even the smallest change of radiation intensity will manifest its quality. Nature itself has created a very sensitive sensor which parameters are about 300 mil. km^2. This imaginary sensor react not only on radiation which creates it, but also on secondary changes, caused for example by high energetic source of radiation gamma (GRB). It is as a huge membrane, which waves in rhytm of solar and cosmic events. Every of these changes can be measured and thereafter evaluated as SID.

Source of radio signal

As a source of radio signal we use one of VLF transmitter network. (Figure 1) How does very low frequencies and astronomy relate to each other? One of the characteristics of VLF is that it is reflecting from D layers of ionosphere. This layer is impermeable for radio waves of very low frequencies up to such an extent that waves are reflected as from a mirror. (Figure 2)This is precisely that characteristic why we use them in this method. Radio waves are repeatedly reflected from D layer of ionosphere and from earth's surface. At sufficient performance of transmitter these radio waves are kept in a waveguide for a distance up to several thousand of kilometres.
Waveguide, which is created from D layer of ionosphere a earth's surface, reacts very sensitevely to changes one of the other party. From outside it is affected by solar activity. There are measurable changes in quality of ionosphere in case, it is affected by high energy gamma rays (GRB). From the earth's surface are the changes induced by the earthquake, storm activity and measured and documented is also acting ionospheric wave induced test nuclear weapons. Any changes in quality of waveguide is immediately registered in intensity of received radio signal.

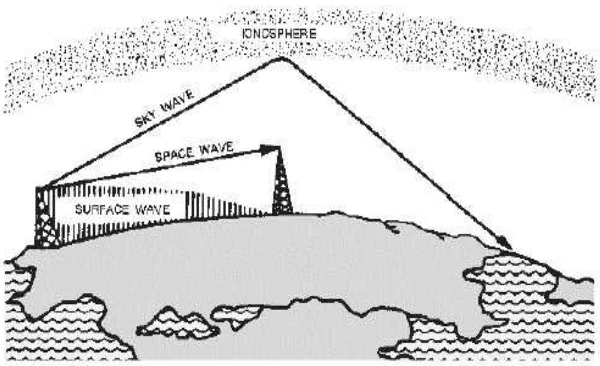

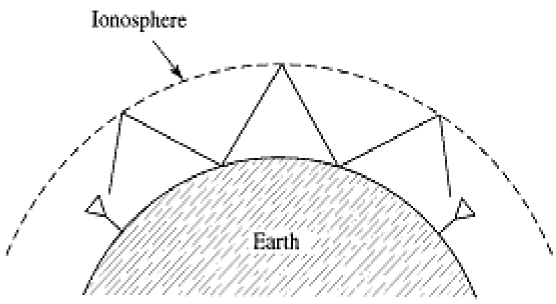

Figure 1, 2

Receiver (SID monitor)

SID monitor consists of three parts. It is a loop antenna. Tuned VLF receiver and analog-digital converter. Revised and converted to digital form signal is brought to the PC and then processed by appropriate software. What is important to say is, that for our measurment, only intensity of carier is important, not the information carried by carrier.

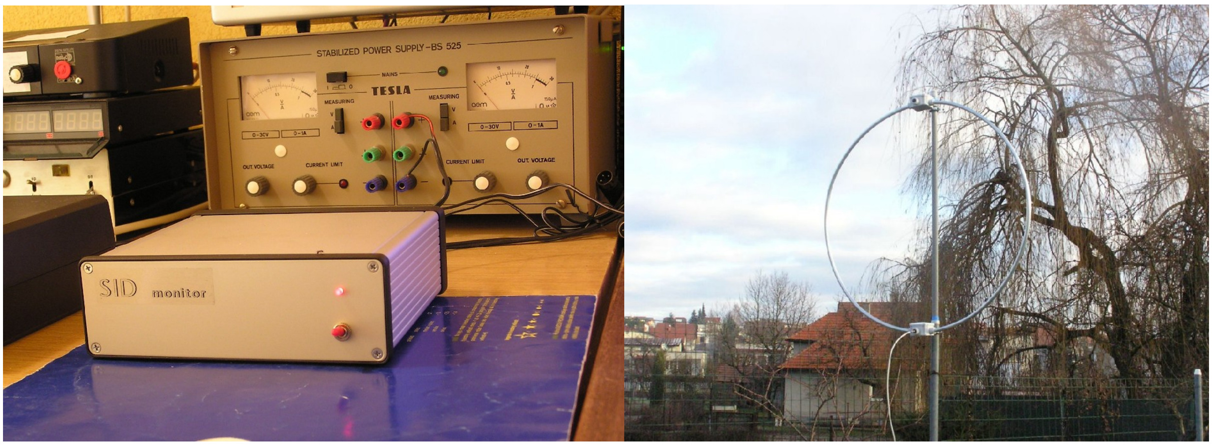

Figure 3, 4: Receiver and anthena

Evalution results

Record of SID monitor during 24 hour period is repeating as if prescribed by a template. (Figure 5) At night the radio waves are reflected by higher layers of the ionosphere and this also correspond to the actual record, which is characterized by rapid changes. The transition between night and day is significant and easily readable record. During the day they are reflections from the D layer of ionosphere. It is made up of direct sunlight so the record corresponds to changes in its intensity. Termination of sunlight will be expressed by considerable change and a smooth transition in to night curve.
These fundamental changes repeats regularly and vary only by change of the length of day and night, influenced by rotation of seasons. Significant changes are also caused by 11 years Solar cycle.

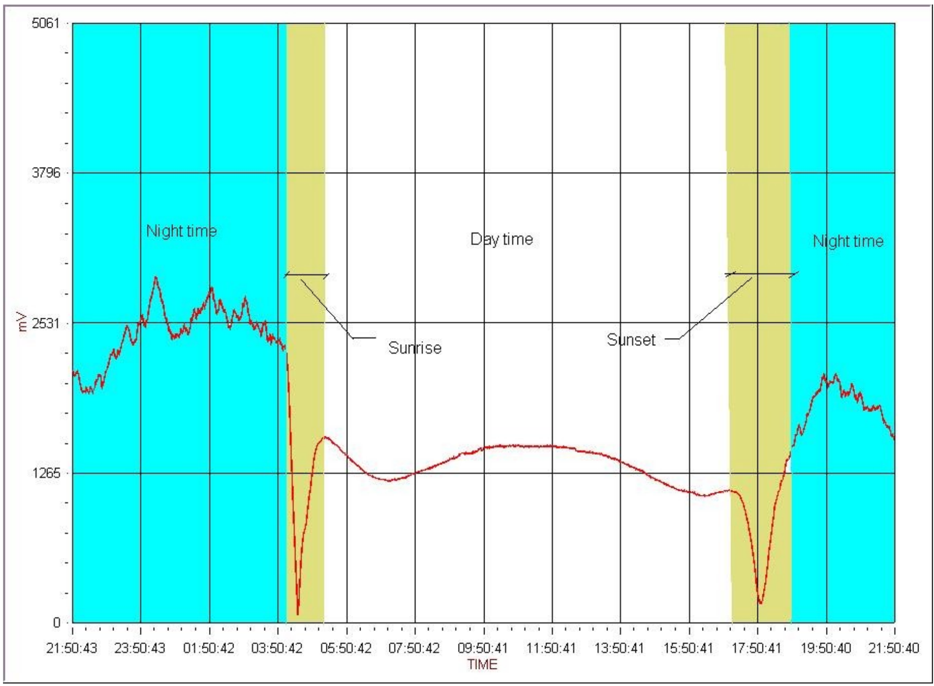

Figure 5: Template of all-day record

Results

The Figure 6 is a record of SID monitor from 6.12.2006. Solar flares reached a flashpoint M6, C6, C2 and C4. Individual peak match with a record of the GOES satellites and demonstrate the possibilities and the sensitivity of this method. Just for comparison and demonstration of possibilities of SID monitor I attach a few examples of positive measurements.

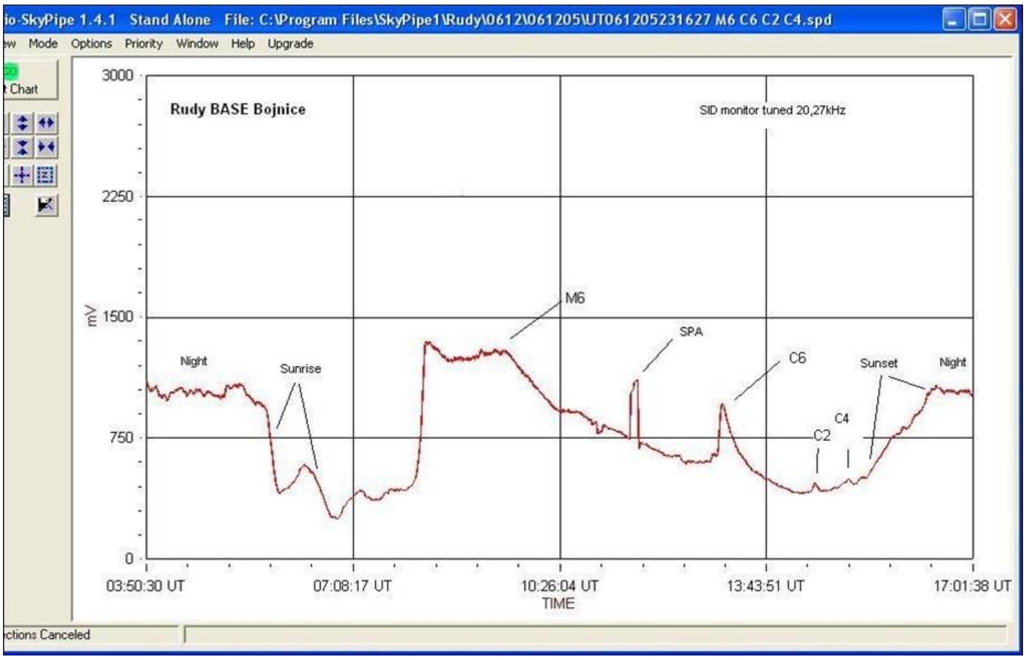

Figure 6: SID monitor record from 6.12.2006

The figure 7, 8 is a record from 5.4.2006 and a record of satellites SOHO beneath.

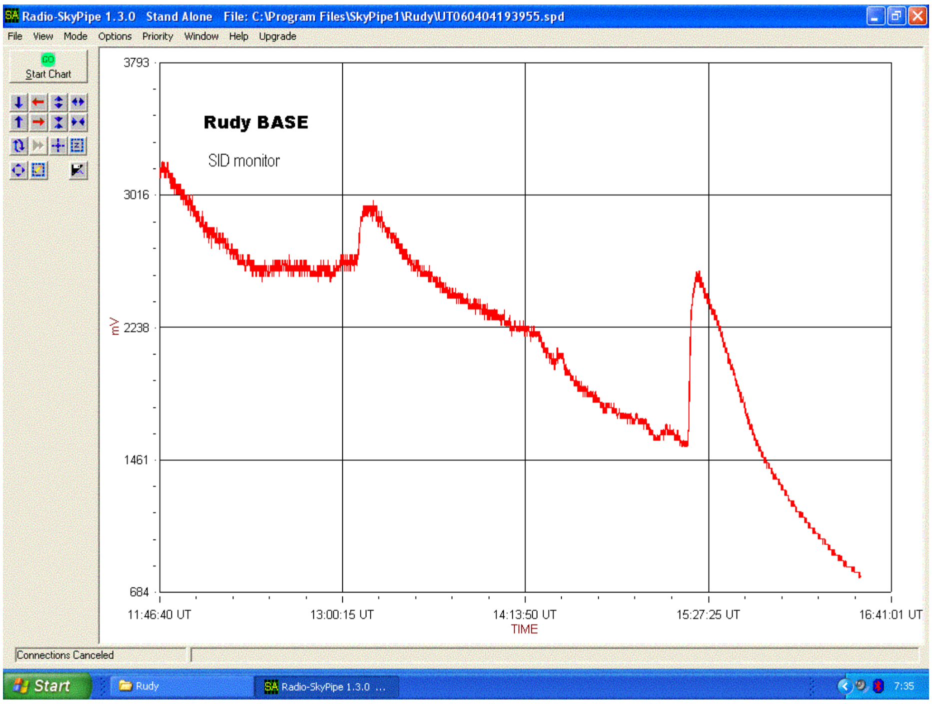

Figure 7: SID monitor record from 5.4.2006

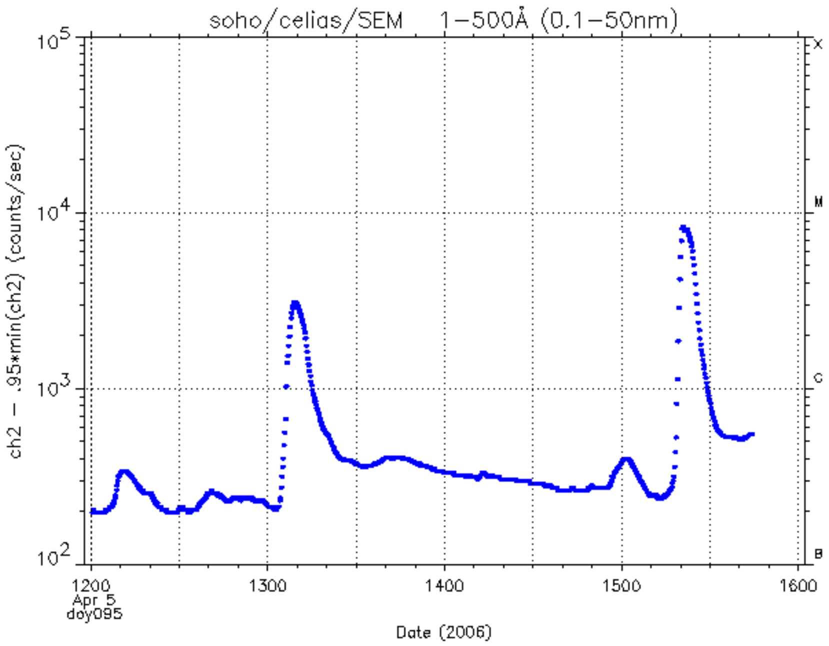

Figure 8: Record of SOHO satellite

Figure 9 shows the record from 3.11.2008. On this record is noticeable peak of Solar flare class B8.

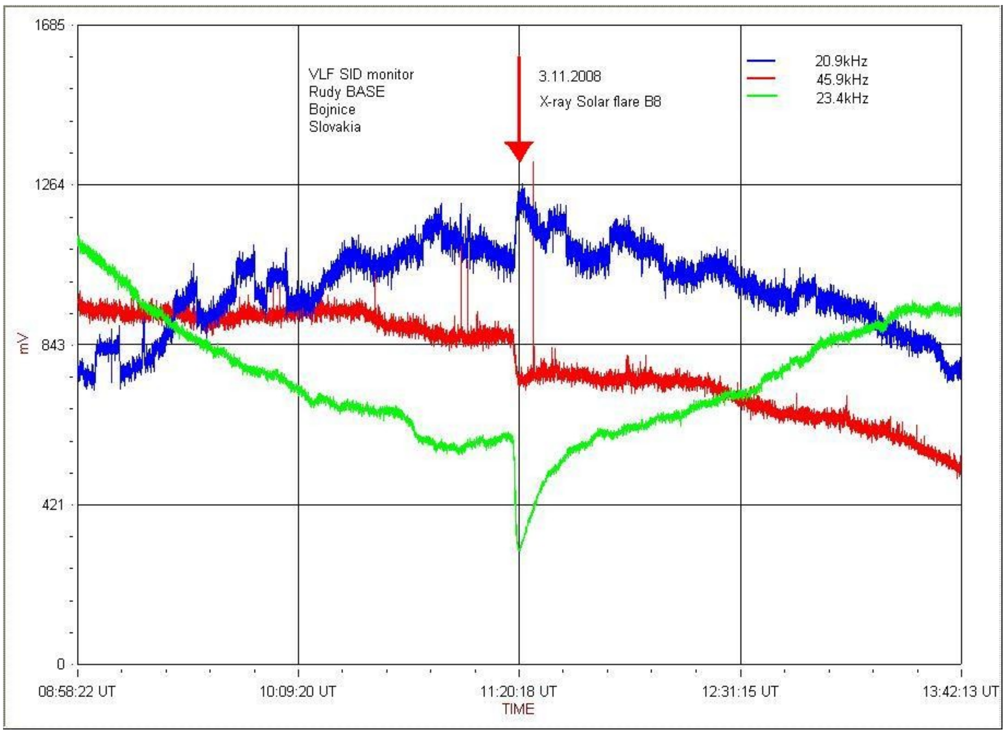

Figure 9: SID monitor record from 3.11.2008

Conclusion

Observation and monitoring of solar flares is just one of the few ways of using the methods of SID monitor. Waveguide, consisting of D layer ionosphere and the Earth's surface, reacts very sensitively to any changes in operating one of the other party. From outside it is affected by solar activity. There are measurable changes in quality of ionosphere in case, it is affected by high energy gamma rays (GRB). From the earth's surface are the changes induced by the earthquake and measured and documented is the wave induced by nuclear weapons test.

References

[1] Space Weather Monitors Stanford Solar Center

[2] AAVSO SID Project

[3] Lionel Lodet SID monitoring station

OPEN EUROPEAN JOURNAL ON VARIABLE STARS
September 2009 http://var.astro.cz/oejv ISSN 1801-5964

The mysterious and complicated interacting binary beta Lyr, new proof of the existence of various structures of a circumstellar matter

P.Chadima[1], P.Harmanec[1,2], H.Ak[3], O.Demircan[3]

(1) Astronomical Institute of the Charles University, V Holešovičkách 2, CZ-180 00 Praha 8, Czech Republic, pavel.chadima@gmail.com
(2) Astronomical Institute of the Academy of Sciences, CZ-251 65 Ondřejov, Czech Republic
(3) Department of Physics, Faculty of Sciences and Arts, Çanakkale Onsekiz Mart University, 17100, Çanakkale, Turkey

Abstract: Beta Lyr is a very complicated and one of the most intensively studied interacting binary. Our study of this eclipsing binary was based on two sets of spectra - 651 "red" electronical spectra and 52 "blue" digitized photographic spectra. They were processed in two different ways. First, we disentangled four appropriate spectral regions into the spectra of both main binary components. Next, we made spectrophotometric measurements and subsequent processing of the 15 pronounced absorption lines belonging to the primary star. Both processing of data led to a finding of new spectral lines, most probably originating in various structures of a circumstellar matter.

Abstrakt: Beta Lyr je velice komplikovaný a jeden z nejvíce studovaných interagujích dvojhvězdných systémů. Naše studie tohoto zákrytového systému byla založena na dvou sadách spekter – 651 „červených" elektronických spektech a 52 „modrých" digitalizovaných fotografických spektech, které byly zpracovány dvěma metodami. Nejprve jsme rozložili čtyři spektrální oblasti na spektra obou hlavních složek dvojhvězdného systému. Dále jsem provedli spektrofotometrické měření a následné zpracování 15 výrazných absorpčních čar příslušejících primární hvězdě. Obě metody vedly k objevu nových spektrálních čar, pravděpodobně pocházejících z různých struktur mezihvědné hmoty.

Introduction

Beta Lyr is an eclipsing and interacting binary which is at the stage of high mass-transfer rate between the components. Circumstellar matter most probably consists of a geometrically and optically thick accretion disk which entirely hides a light from the secondary, jet-like structures perpendicular to the orbital plane and a scattering gas envelope surrounding the disk around the secondary. (See Harmanec (2002) and references therein for more details and a history of investigation of beta Lyr.)
In the present study, we used two sets of spectra – 52 "blue" digitized photographic spectra secured at the Ondřejov Observatory, Czech Republic and 651 "red" electronic spectra, secured at Ondřejov and at the Dominion Astronomical Observatory, Canada.

Disentangling the spectra

Disentangling the spectra was carried out using the program KOREL (Hadrava 2004). Our results are presented in Figure 1. For electronic spectra, it was necessary to include telluric lines which appear in the given spectral region. One can see that the disentangling led to the discovery of a number of weak absorption lines originating in the pseudophotosphere of the accretion disk. In other words, we obtained a rich line spectrum of the disk, not limited to previously known two silicon lines seen in the fourth panel. Emission lines seen in the disk spectra originate actually in the jet-like structures but we were not successful in separating them from these spectra. Primary spectrum corresponds quite well to the synthetic spectrum with T=13000K, log g=2.5[cgs] and v.sin(i)=55km/s which agrees with the values currently adopted for this star. Such a comparison for the disk spectrum is complicated since there are still no synthetic spectra for accretion disks. However, radial velocities for the accretion disk spectra define well a sinusoidal RV curve in antiphase to that for the primary.

Spectrophotometry of absorption lines

Central intensity (CI) and equivalent width (EW) of 15 pronounced absorption lines was measured on the source spectra. A problem is that these lines originate in the primary but their quantities are measured with respect to the continuum of both the primary and the accretion disk. It is obvious that the measured quantities must be corrected to the continuum of the primary star only. To do such a correction, one needs to have a synthetic light curve of the whole binary and of the primary only (due to eclipses by the accretion disk) since this correction depends on the ratio of these two quantities in given orbital phase. For such a modeling, we used program Binsyn, developed by A.P.Linnell (2000).

In Figure 2, there are phase plots of observed and corrected CI and EW of Si II 6371 line. One can see very pronounced line strengthening in the phases round a primary eclipse. The same phase dependence was found also for all other investigated lines. These changes are too large to be caused by physical or geometrical properties of the primary. This effect can be also demonstrated in Figure 3. Note that the absorption lines in the phase of primary mid-eclipse (second spectrum) are deeper which is in the contradiction with the fact that most of the primary surface is hidden from view in this phase.

It seems that the only plausible explanation is this one: During the eclipse, there is always a certain part of the primary which remains uneclipsed by the disk and the light from this uneclipsed part goes though both, one of the jets and the gas envelope toward an observer. These circumstellar structures may cause an additional absorption. If correct, this interpretation means that there is another absorption line spectrum observable only in the phases of the primary eclipse.

Conclusion

Both analyses led to the discovery of a new set of spectral lines – an accretion disk spectrum and an „eclipsing“ spectrum. Presence of these spectra supports the current model of beta Lyr with the accretion disk, the jet-like structures and the scattering envelope above the disk. Further analysis of these spectra could bring new pieces of information about this enigmatic binary. A detailed discussion of this spetral study can be found in the paper Ak et al. (2007).

Acknowledgement

We acknowledge the use of the programs SPEFO, BINSYN and KOREL, made available by their authors J.Horn&J.Krpata, A.P.Linnell&I.Hubeny and P.Hadrava respectively. Our special thanks go to A.P.Linnell for his patient advice concerning the proper use of BINSYN. Some of the Ondřejov spectra were obtained by P.Hadrava, D.Holmgren, J.Horn, J.Kubát, V.Šimon and S.Štefl. We profitted from the use of electronic bibliography maintained by the NASA/ADS systém. Czech authors were supported from the research plans J13/98: 113200004 of Ministry of Education, Youth and Sports and AV 0Z1 003909, from project K2043105 of the Academy of Sciences of the Czech Republic and from the grants GA~ČR 205/02/0788 and GA~ČR 205/06/0304 of the Granting Agency of the Czech Republic. Turkish authors were partly supported by the Research Council of Turkey and the Research Foundation of Çanakkale University. Collaboration between Turkish and Czech authors was facilitated thanks to a NATO collaborative linkage grant PST.CLG.979343.

References:

Ak et al. 2007, A&A, 463, 233

Hadrava, P. 2004, Publications of Astron. Inst. of the CAS, 92, 15

Harmanec, P. 2002, Astronomische Nachrichten, 323, 87

Linnell, A.P. 2000, MNRAS, 319, 255

Attachements

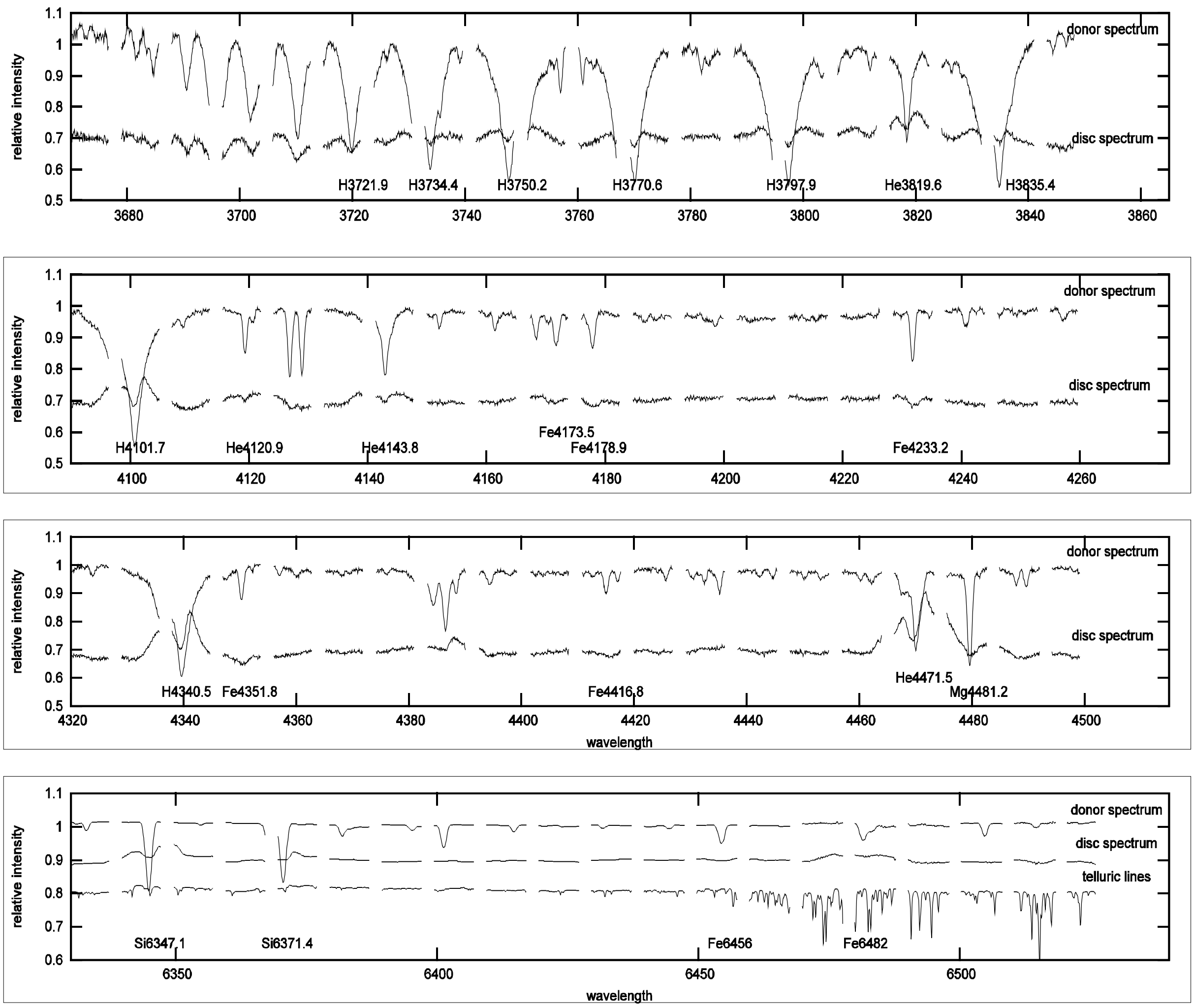

Figure 1: Disentangling of four spectral regions. Emission lines, seen in the disk spectra, originate in fact in the jet-like structures but our attempt to disentangle them separately failed.

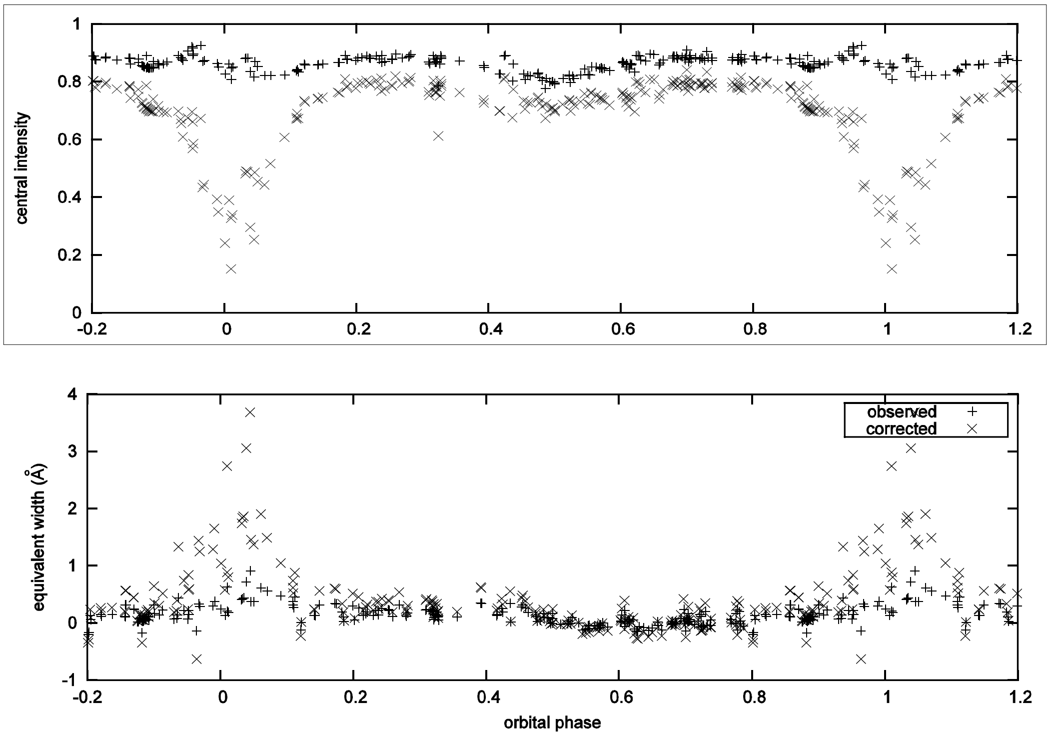

Figure 2: Phase dependency of central intensity and equivalent width of Si II 6371 line. Observed values are shown as +, corrected values as ×.

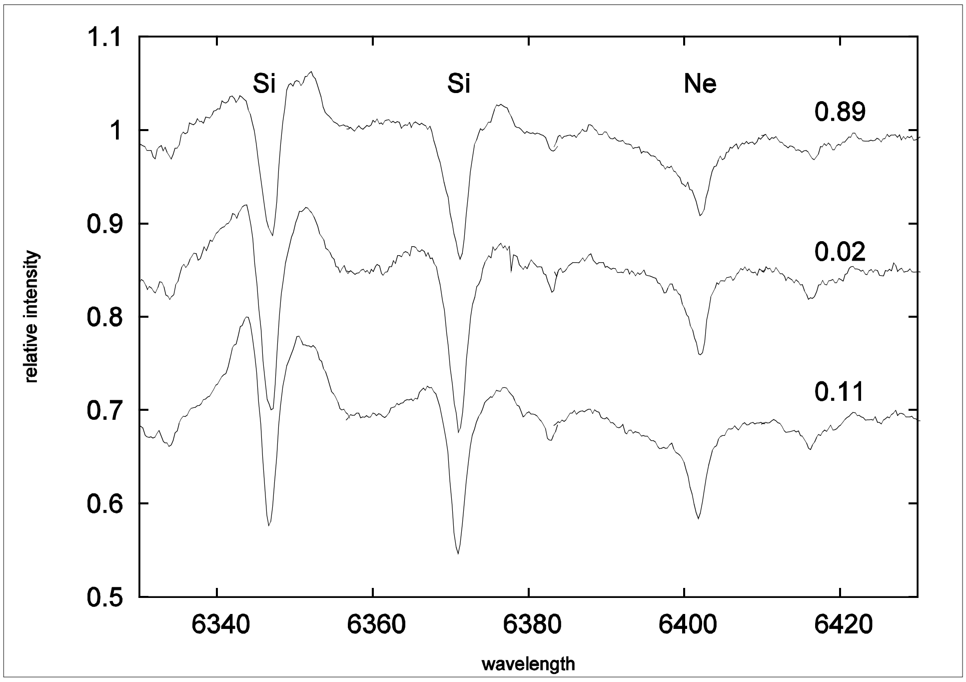

Figure 3: Three spectra around the primary eclipse. Orbital phases are given on the right side.

OPEN EUROPEAN JOURNAL ON VARIABLE STARS
September 2009 http://var.astro.cz/oejv ISSN 1801-5964

The O-C gate

ANTON PASCHKE

Abstract: A short history and a description of the O-C GATE database is given.

Abstrakt: Tento příspěvek přináší krátký vhled do historie vývoje O-C brány a její stručný popis.

History

Since the time of prof. Oburka it was recommendet to observe neglected stars and to avoid stars that have been already frequently observed. There was a system of so called Mikulasek-points valuating the observed results with 1 to 10 points. Obervers should seek to achieve a maximum of points.
With personal computers (Apple II) available it was possible to collect published minima and present reasonable statistics, rhather then just to guess the amount of known minima. It became also easy to draw O-C diagrams and to correct elements.
The collection of the data from literature was done by several people. I would like to mention Francesco Acerbi, Massimiliano Martignoni and Ivan Andronov, who collected a part of the data now stored in O-C GATE.
The first, who begun the collection of data was indeed Dieter Lichtenknecker. His collection is still maintained by the BAV. There was also a collection of data by dr Kurpinska-Winarska, the editor of the well known SAC. Due to her health problems and her retierement only a preliminar version of the database reached the internet. A larger database is maintained by prof Kreiner, also in Krakow. Unfortunaltely, only diagrams and not numbers (minima times) are available on the internet.
The Lichtenknecker database was available on CD, but not in the internet at the time we introduced the O-C GATE homepage. A large number of minima from the CD was used by us. We had the minima, but without literature references and (some until now) without the name of the observer. We, mainly Martignoni, had collected also RR maxima timings. They are now presented in the GEOS RR-Lyrae database.

The aims of the O-C GATE

- to identify and observe neglected stars
- to ensure, that elements used for forecasts are reasonable
- to check the plausibility of the minima prior to publishing
- to be a starting point for deeper studies. But students should be advised to seek and read the original papers. The tabular form of a database can not contain all the information shared by the observer. Unfortunately, the literature reference is still a weak point of O-C GATE.

What stars should be included in O-C GATE?

In principle: eclipsing stars. But there are stars with doubts about the classification, both minima and maxima are found in literature. There are some HADS stars, frequently observed by amateurs, but rejected by the GEOS RR-Lyr database (as they are not RR Lyr stars).
It makes little sense to just copy the information from the GCVS. So we insert only such stars, where we have additional information, compared to the GCVS. New naming lists do not contain elements, therefor the stars are included in O-C GATE, even if only one minimum is known. Some stars with provisional designations are included.
As soon as the GCVS editors will asign a definitive name they will be deleted and inserted again with the definitive name. That means doubled work. There is some danger, that we will exclude a star now and soon regret the exclusion because observers become interested exactly on that star. Eclipsing dwarf nova may be such cases.

The principles used to determine the elements

This is the central part of paper! I am applying only one principle: the O-C diagram should look reasonable. The elements giving a pretty diagram are not necesserly the same that give an exact forecast! It is better to calculate the forecst from the last relaible minimum. Explicitly I do not seek elements, where the last part of the O-C point-clound would aproach the X-axis tangentialy. That is atempted by most competitors, sometimes with spectacular failure. Some examples illustrated this part of the lesson, but they should not be repeated here: RR Dra, IV Cas, OX Cas, PV Cas, FT Ori, SW Oph, V 995 Cyg.

The meaning of some fields in the tables

JC and JD: in the past I used Turbo Pascal. That programming environment used (in absence of a 8087 coprocessor) the 48 bit Borland-arithmetics. It was not able to calculate julian data with 5 decimal digits. Consequently the most significant digits, always 24, sometimes 23, where stored separately. The IEEE 64-bit arithmetic used now can handle the numbers, but in printed form the 24 is often omitted as well.
The field ERROR should contain a guess of the distante between the point and a somehow defined middle-line in the O-C diagram. It should not be, but is, a measure of the prestige claimed by the observer.
The field OBSERVER. Coming from the tradition of visual observation we can have exactly one observer. Papers may have several authors, data may be observed by satellites, we have one observer!
The same observer may operate two or more telescopes with ccd cameras, different workers may use the same archived photographic plates. Some sky surveys are operated over years. A minimum derived from such data should have a defined observing season. This is seldom explicitly published and has no field in the database.
The student using O-C GATE should read the original papers!
The field TYPE should specify the GCVS conform type of the star: EA, EB, EW, EP, ELL, eventually with subtype, like EW/KW or in case of doubt EW, RRc In fact the most frequent value is "empty". The field was introduced as the database already existed and contained many stars.
The brightness of the stars is a complex difficulty for our collection. First one has to define the color. Generaly Johnson filters B and V are referenced, older observations have "pg" for photographic plates. Newer measurements have "ccd" for unfiltered ccd. But what is the difference between V and ccdV ? Between -Ir and Ic ?
The second great problem is, that the secondary minima are described in the remarks (and not in the main table) of the GCVS. So they had not been included in the older versions of the O-C GATE. Later the field was created, but used to be empty. For EW stars it is reasonable to assume secondary minima similar to primary, but the update was made for all stars. So for EA stars the secondary minimas magnitude may be grossly wrong.
Another point of the ongoing discussion is, that amplitude is easy to determine, but magnitudes not.
A revision of this part of the database is under way.
Some more fields may be desirable. Many eclipsing pairs have further compagnions. The closest may manifest their presence by the light time effect in the O-C diagram. Sub-arcsecond compagnions may decrease the amplitudes, very close visual binaries may confuse photometry programs. Such stars may require special equipment, common, today increasingly popular short focal length optics may lead to unstatisfactory results. Therefore the distance between the components of a visual binary would be an usefull selection criterium aplied in the minima forecast. Similar to limiting magnitude or height above horizont already used.

Maintenence of the database

The database has no versions. Any published list of minima is included as soon as possible, as the workload permits. Mainly journals available in the internet are used. Minima published in prestigious journals (not available for free) have a great chance to be missed. Not yet published observations, communicated to me, may be inserted into the database, if they prove a correction of the elements. The observers should not vaste precious time by using obsolete elements. But generaly the minima should first be published and then inserted into O-C GATE, with an understandable literature reference.

OPEN EUROPEAN JOURNAL ON VARIABLE STARS
September 2009 http://var.astro.cz/oejv ISSN 1801-5964

The strange optically variable source SWIFT J195509+261406 and implication for optical observers

RENÉ HUDEC AND VOJTĚCH ŠIMON *on behalf of* ALBERTO J. CASTRO-TIRADO & COLLABORATION

A.J. CASTRO-TIRADO [1], A.DE UGARTE POSTIGO [2,1], J. GOROSABEL [1], M. JELÍNEK [1], T. A. FATKHULLIN [3], V. V. SOKOLOV [3], P. FERRERO [4], D. A. KANN [4], S. KLOSE [4], D. SLUSE [5], M. BREMER [6], J. M.WINTERS [6], D. NUERNBERGER [2], D. PÉREZ-RAMÍREZ [7], M. A. GUERRERO [1], J. FRENCH [8], G. MELADY [8], L. HANLON [8], B. MCBREEN [8], K. LEVENTIS [9], S. MARKOFF [9], S. LEON [6], A. KRAUS [10], F. J. ACEITUNO [1], R. CUNNIFFE [1], P. KUBÁNEK [1], S. VÍTEK [1, 20], S. SCHULZE [4], A. C. WILSON [11], R. HUDEC [12, 20], V. ŠIMON [12], J. M. GONZÁLEZ-PÉREZ [13], T. SHAHBAZ [13], S. GUZIY [14], S. B. PANDEY [15], L. PAVLENKO [16], E. SONBAS [17], S. TRUSHKIN [3], N. BURSOV [3], C. SÁNCHEZ.-FERNÁNDEZ [18] & L. SABAU-GRAZIATI [19]

(1) IAA-CSIC, Camino Bajo de Huétor, 50, E-18008 Granada, Spain
(2) ESO, Alonso de Córdova 3107, Vitacura, Santiago, Chile
(3) SAO-RAS, Nizhnij Arkhyz, Karachai-Cirkassian Rep., 369167 Russia
(4) Thüringer Landessternwarte Tautenburg, Sternwarte 5, D-07778 Tautenburg, Germany
(5) Laboratoire d'Astrophysique, EPFL, Observatoire, 1290 Sauverny, Switzerland
(6) IRAM, 300 rue de la Piscine, 38406 Saint Martin d'Héres, France
(7) Facultad de Ciencias Experimentales, Universidad de Jaén, Campus Las Lagunillas, E-23071 Jaén, Spain
(8) School of Physics, University College, Dublin, Ireland
(9) Astronomical Institute 'Anton Pannekoek', Univ. of Amsterdam, The Netherlands
(10) MPI fur Radioastronomie, Bonn, Germany
(11) Department of Astronomy, University of Texas, Austin, TX 78712, USA
(12) Astronomical Institute of the Czech Academy of Sciences, Ondrejov
(13) IAC, Vía Láctea s/n, La Laguna, Tenerife, Spain
(14) Nikolaev State University, Nikolskaya 24, 54030 Nikolaev, Ukraine
(15) ARIES, NainiTal, India
(16) Crimean Astrophysical Observatory, Nauchnyv, Ukraine
(17) Univ. of Cukurova, Dep. of Physics, Adana, Turkey
(18) ESAC Villafranca del Castillo (Madrid), Spain
(19) INTA, Ctra. de Ajalvir km. 4, 28750 Torrejón de Ardoz (Madrid), Spain
(20) Czech Technical University in Prague, Faculty of Electrical Engineering, Prague, Czech Republic

---

The GRB & optical counterpart of SWIFT J195509+261406

- Detected on 10 June 2007 20:52:26 UT by *Swift*/BAT as a normal single-peaked long burst, indistinguishable from cosmic GRBs (Pagani et al. GCN 6489) at galactic coordinates (l , b) = (63.5, -1.0)
- Stefanescu et al. (GCN 6492) reported the detection of a variable optical counterpart.
- de Ugarte Postigo et al. (GCN 6501) confirmed the detection with observations from the 1.5m OSN.
- D.A. Kann et al. (GCN 6505) suggested a Galactic origin, based on unusual flaring activity and location near the galactic plane: l=63.3° b=-1°
- Dubbed SWIFT J195509+261406.

Our dataset

Between 1 minute and 1 year after the burst:

- Radio observations from RATAN-600 and 100m Effelsberg
- Millimetre observations from Plateau de Bure & IRAM
- NIR imaging from 8.2m VLT (including AO)
- Optical data from 1.5-m OSN, 0.3-m BOOTES-2, 0.4-m WATCHER, 1.34-m TLS, 6.0-m BTA and 8.2-m VLT
- X-ray data from *Swift*/XRT & *XMM-Newton*

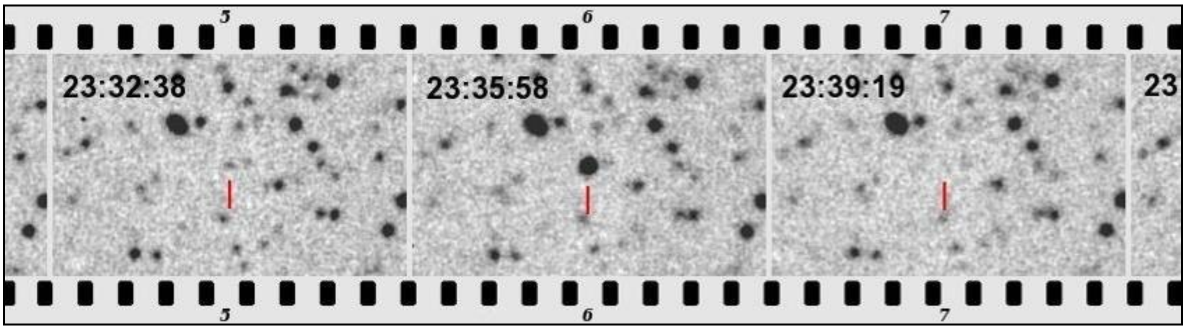

Figure 1: The early optical flaring activity of SWIFT J195509+261406

Early optical light curve

- We recorded ~ 40 flare episodes
- Up to I~14.8, timescales of ~20sec - 7 min
- Amplitudes up to 7 mag

Late flare (June 21/22 VLT Near-IR flare)

- After the third day activity decreases
- A faint source was still detectable
- Last flare is detected 11 days after

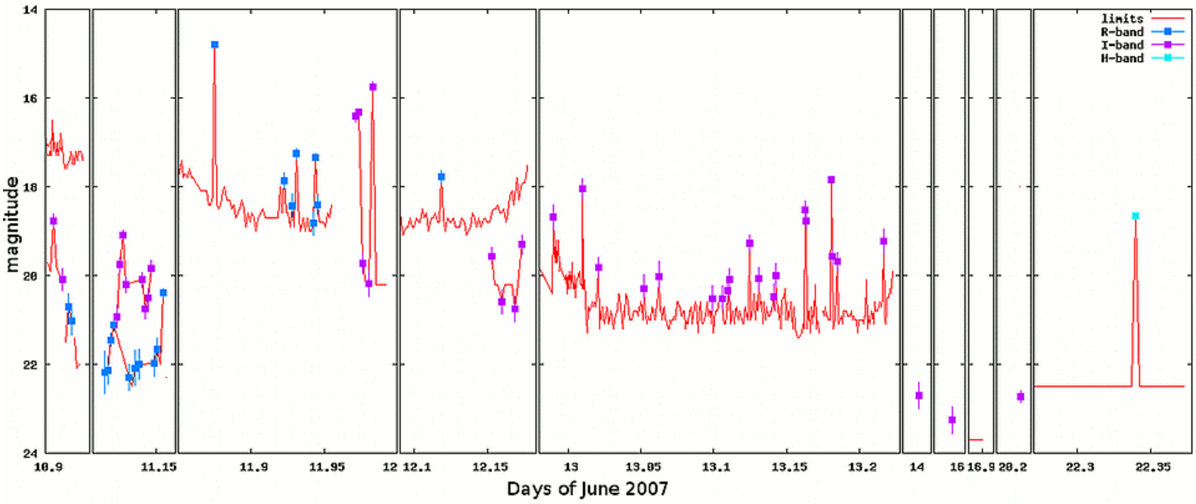

Figure 2: Total (of our collaboration) optical light curve of the flaring counterpart.

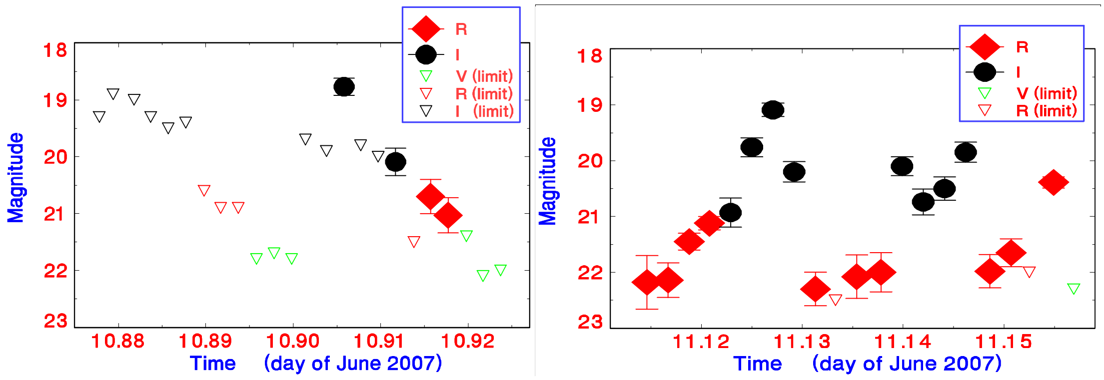

Figure 3: Left: An example of a dense series of *VRI* observations (duration ~75 min) (June 10, 2007). J1955 was near the detection limit, but peaks of several flares are resolved. Amplitude of the brightest *R* band flare is > 1 mag(*R*). Baseline brightness is below the detection limit.

Right: Dense series of *VRI* observations (duration ~65 min) (June 11, 2007). J1955 was clearly detected. The *I* and *R* data are not quite simultaneous. Significant fluctuations of the brightness are apparent (~1 mag, timescale ~15 min). Baseline brightness is well-defined both in *R* and *I*.

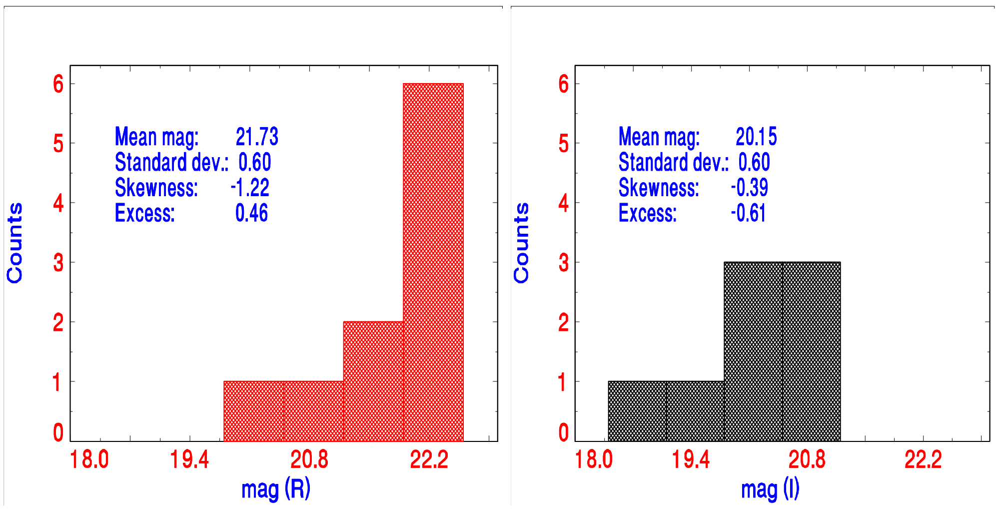

Figure 4: Statistical distribution of *R* and I magnitudes in the June 11 series (left). The most abundant faintest magnitude and negative skewness imply that the observed brightness fluctuations have the form of peaks (spikes) from a well-defined baseline brightness. The mutual similarity of the statistical distributions of *R* and *I* magnitudes in this night series enables to determine the mean color index *R-I* from the mean mag in each filter.

Right: Comparison of the color index *R-I* from the June 11 series with the color of OAs of GRBs from Simon et al. (2004). Colors of the ensemble are de-reddened for the Galactic extinction and are in the observer frame. The color of J1955 was dereddened by A_V = 4 mag, near the lower limit A_V=3.6 mag of the suggested range. Further increase of A_V leads to the decrease of the color index (arrow). $(R\text{-}I)_0$ of J1955 is thus similar to that of the ensemble of OAs and is consistent with the synchrotron emission (e.g. Sari et al. 1998). Thus thermal emission is ruled out.

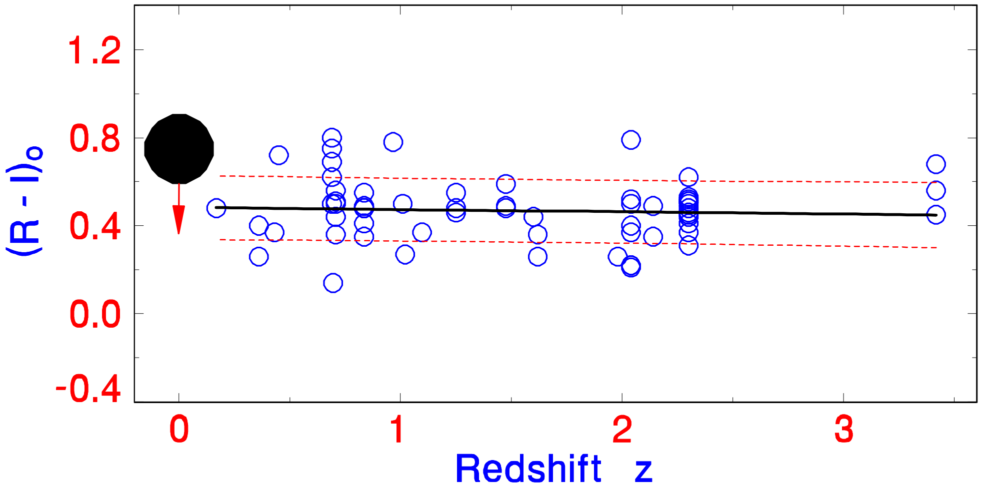

Figure 5: Comparison of the color index *R-I* from the June 11 series with the color of OAs of GRBs from Simon et al. (2004). Colors of the ensemble are de-reddened for the Galactic extinction and are in the observer frame. The color of J1955 was dereddened by A_V = 4 mag, near the lower limit A_V=3.6 mag of the suggested range. Further increase of A_V leads to the decrease of the color index (arrow). $(R\text{-}I)_0$ of J1955 is thus similar to that of the ensemble of OAs and is consistent with the synchrotron emission (e.g. Sari et al. 1998). Thus thermal emission is ruled out.

Baseline flux evolution

- The emission between flares slowly decreased until it disappeared.
- No detectable quiescent counterpart once the flaring emission ceased
- Limits: H, I > 23 (VLT, our work), R > 26.5 (Keck, Kasliwal et al. paper, ApJ 2008), and I > 24.5 (Keck, Kasliwal et al. paper, ApJ 2008)

Distance scale

- X-ray → $N_H=(7.2^{+3}_{-2})$ x $10^{21}cm^{-2}$ → A_V=3.6 – 7.5 mag
- H I observations
  → $N_{H\,I}$ = (8.1±1.2) x $10^{21}cm^{-2}$

Observational facts

- Gamma-ray burst-like “event” triggering the activity
- X-ray, optical and nIR (but no radio) flaring events
- X-ray and optical baseline emission detected as well *between* the flares but no at radio or soft (15-40 keV) gamma-rays.
- Dramatic optical flaring activity for ~2 days
- No quiescent counterpart once the activity ceased (only deep limits in radio, NIR & X-rays)
- Galactic origin

What is the nature of the source ?

- GRB?
- Light curve behaviour and location rule it out.
- A "fast X-ray nova"? (Uemura et al. 1999, Kasliwal et al. 2008)
- Unlike V4641 Sgr, where strong gamma-ray and radio emission was detected (reaching around 1 Crab in gamma-rays and few mJy in radio, compared to < 0.01 Crab and < 0.1 mJy respectively for the SWIFT source).
- Bursting pulsar?
- GRO J1744-28, where further gamma-ray activity was observed, is also quite different. No pulsations measured in the SWIFT source for the time being.
- An ultra-compact low-mass X-ray binary?

Flares could be produced by blobs of homogeneous synchrotron-emitting plasma of size of 10^7 cm and magnetic field of strength 10^5 G.

The blobs can be found in a magnetized corona (Merloni et al. 2000) or a wind (rather than in the outer regions of a collimated jet).

- A soft gamma-ray repeater?
- SGRs are magnetars (young NS with B = 10^{14-15} G) with a prolific bursting rate when they are "switched-on".
- Flares would be due to coherent plasma bunches (Thompson & Beloborodov 2005), leading easily to the observed optical luminosities of : 10^{35} (D/5 kpc)^2 erg/s

SGR hypothesis is supported by:

1. the lognormal distribution burst fluxes.
2. similarities with other *transient* magnetars: harder, intermediate-duration bursts with comparable energy releases to GRB 070610 also observed in magnetar, similar X-ray decaying light curves
3. a possible periodicity in the X-ray data (Kasliwal et al. 2008, Stefanescu et al. 2008): similar period as seen in other magnetars (few s)

Implications

- A *new* magnifestation of magnetar activity, becoming one of the few hundred Galactic ones becoming active in 10^4 yr.
- The quiescent X-ray luminosity :

$$L_x < 9 \times 10^{31} (D/5\ \mathrm{kpc})^2\ \mathrm{erg/s}$$

is intermediate between transient magnetars (including SGRs/AXPs):

$$L_x = (2\text{-}4) \times 10^{35}\ \mathrm{erg/s}$$

and dim isolated neutron stars (DINs):

$$L_x = (2\text{-}20) \times 10^{30}\ \mathrm{erg/s}$$

- The missing link between magnetars and DINs ?

Implications for optical observers

It is evident that we have observed a new type of galactic optically variable object. The strange pattern of optical variability is different from all the objects astronomers have observed, as optically variable objects, before. With maximum of I ~ 15, the object was accessible to small telescopes.
First we have to stress the importance of robotic optical telescopes, as they have contributed essentially to this discovery. Albeit some similar objects may be fainter, the flaring object discussed here was well within the range of small aperture telescopes.
The detection of nearly 40 flaring optical episodes, delayed to the gamma-ray emission, from the source which may be galactic magnetar, has the following consequences.

1. It is justified to observe the positions of GRBs for prolonged periods after the GRB times (at least for targets close to galactic equator), even in the case when there was no OA observed immediately after the GRB time.

2. It has sense to follow-up GRBs occurring near Galactic equator, despite of the high galactic extinction expected, and despite the fact that the rate of occurrence of objects analogous to SWIFT J195509+261406 is unknown, and may be very low.

3. As the target may be galactic magnetar, future activity periods may occur. This means that (robotic) optical observations of the target position could reveal possible recurrence. This is however still difficult as the flares are short and the recurrence duty cycle unknown. However, design and development of novel automated observing devices and cameras for these goals may be considered.

4. The field of optical counterparts to GRBs can still provide more unexpected discoveries.

5. Triggers similar to the observed ones may be recorded in various databases, e.g. astronomical plate archives. This means that the detailed and extended data mining in large observational datasets with deep limiting magnitudes may give quite interesting results.

Conclusions

- We observed a normal GRB and found a peculiar galactic source (b = -1.0) with intense flaring activity.
- Optical flares of over 4 magnitudes and durations of ~1 min (not observed in "classical SGRs", not only a "high Galactic extinction" problem).
- This confirms the important role of automated robotic telescopes and cameras.
- An ultracompact LMXB?
- The fifth SGR in the Galaxy? First optical counterpart detected for such object.
- The missing link between magnetars and DINs?
- The object represent an yet unknown representation of optical variability, different from all galactic variable objects observed before.

Acknowledgements

We acknowledge the support provided by the ESA PECS Project 98023 and by the Grant Agency of the Czech Republic, grant 205/08/1207.

References

[1] Thompson, C. & Duncan, R. C. The Soft Gamma Repeaters as Very Strongly Magnetized Neutron Stars. II. Quiescent Neutrino, X-Ray, and Alfven Wave Emission, Astrophys. J. 473, 322-342 (1996).

[2] Mazets, E. P., Golenetskii, S. V., Gurian, Iu. A. & Ilinskii, V. N. The 5 March 1979 event and the distinct class of short gamma bursts: Are they of the same origin? Astrophys. and Sp. Sci. 84, 173-189 (1982).

[3] Kouveliotou, C. et al. The Rarity of Soft Gamma-Ray Repeaters Deduced from Reactivation of SGR 1806-20, Nature 368, 125-127 (1994).

[4] Hurley, K. The 4.5±0.5 Soft Gamma Repeaters in Review, in Gamma-Ray Bursts, 5th Huntsville Symposium, Huntsville, Eds. R. M. Kippen, R.S. Mallozzi, and G. J. Fishman, AIP Conf. Proc. 526, 763-770 (2000).

[5] Tueller, J., Barbier, L., Barthelmy, S. D. et al. GRB 070610, Swift-BAT refined analysis, GCN Circ. 6491 (2007).

[6] Pagani, C. & Kennea, J. A. GRB 070610; Swift-XRT position, GCN Circ. 6490 (2007). 9

[7] Kasliwal, M. M. et al. GRB 070610: A curious galactic transient, Astrophys. J. 678 1127-1135 (2008).

[8] Stefanescu, A. et al. Very fast optical flaring from a possible new Galactic magnetar, Nature, submitted (2008).

[9] de Ugarte Postigo, A., Castro-Tirado, A. J. & Aceituno, F. GRB 070610: Optical observations from OSN, GCN Circ. 6501 (2007).

[10] Kann, D. A., Wilson, A. C., Schulze, S. et al. GRB 070610: TLS RRM sees flaring behaviour - Galactic transient?, GCN Circ. 6505 (2007).

[11] Kouveliotou, C. et al. A new type of transient high-energy source in the direction of the Galactic Centre, Nature 379, 799-801 (1996).

[12] Sazonov, S., Sunyaev, R. & Lund, N. Super-Eddington X-ray Luminosity of the Bursting Pulsar GRO J1744-28: WATCH/GRANAT Observations, Astronomy Letters 23, 326-334 (2005).

[13] Markwardt, C., Pagani, C., Evans, P. et al. SWIFT J195509.6+261406 / GRB 070610: A Potential Galactic Transient, Astronomer´s Telegram 1102 (2007), 10

[14] Revnivtsev, M., Gilfanov, M., Churazov, E. & Sunyaev, R. Super-Eddington outburst of V4641 Sgr, Astron. Astrophys. 391, 1013-1022 (2002).

[15] Uemura, M. et al. The 1999 Optical Outburst of the Fast X-Ray Nova, V4641 Sagittarii, Publ. Astron. Soc. Japan 54, 95-101 (2002).

[16] Hjellming, R. M. et al. Light Curves and Radio Structure of the 1999 September Transient Event in V4641 Sagittarii (=XTE J1819-254=SAX J1819.3-2525), Astrophys. J. 544, 977-992 (2000).

[17] Dahn, C. C. et al. Astrometry and photometry for cool dwarfs and brown dwarfs, Astron. J. 124, 1170-1189 (2002).

[18] in't Zand, J. J. M., Jonker, P. G. and Markwardt, C. B. Six new candidate ultracompact X-ray binaries, Astron. Astrophys. 465, 953-963 (2007).

[19] Merloni, A., Di Matteo, T. & Fabian, A. C., Magnetic flares and the optical variability of the X-ray transient XTE J1118+480, Monthly. Not. Roy. Astron. Soc. 318, L15-L19 (2000).

[20] Thompson, C. & Beloborodov, A. M., High-Energy Emission from Magnetars, Astrophys. J. 634, 565-569 (2005).11

[21] Woods, P. M. et al. Discovery of a new soft gamma-ray repeater, SGR1627-41, Astrophys. J. 519, L139-142 (1999).

[22] Ibrahim, A. I. et al. Discovery of a transient magnetar: XTE J1810-197, Astrophys. J. 609, L21-24 (2004).

[23] Mereghetti, S., Esposito, P. & Tiengo, A. XMM-Newton observations of soft gamma-ray repeaters, Astrophys Space Sci 308, 13-23 (2007).

[24] Treves, A., Turolla, R., Zana, S. & Colpi, M. Isolated neutron stars: accretors and coolers, Publ. Astron. Soc. Pacific 112, 297-314 (2000).

[25] Muno, M. P. et al. A search for new Galactic magnetars in archival Chandra and XMM-Newton observations, Astrophys. J. 680, 639-653 (2008).

[26] The SGR/AXP online catalog provided by the McGill Pulsar Group is available at http://www.physics.mcgill.ca/_pulsar/magnetar/main.html .

[27] Israel, G. et al. Discovery and monitoring of the likely IR counterpart of SGR 1806-20 during the 2004 gamma-ray burst-active state, Astron. Astrophys. 438, L1-L4 (2005).12

[28] Hurley, K., McBreen, B., Delaney, M. & Britton, A. Lognormal Properties of SGR 1806-20 and Implications for Other SGR Sources, Astrophys. Space Sci. 231, 81-84 (1995).

[29] Göğüş, E. et al. Statistical Properties of SGR 1900+14 Bursts, Astrophys. J. 526, L93-96 (1999).

[30] Woods, P. M. et al. Hard burst emission from the soft gamma repeater SGR 1900+14, Astrophys. J. 527, L47 (1999).